Published in final edited form as:

J Physiol. 2023 June ; 601(11): 2189–2216. doi:10.1113/JP282273.

Phytochemical compound PB125 attenuates skeletal muscle mitochondrial dysfunction and impaired proteostasis in a model of musculoskeletal decline

Robert V. Musci[1,*], **Kendra M. Andrie**[3], **Maureen A. Walsh**[1], **Zackary J. Valenti**[1], **Melissa A. Linden**[1], **Maryam F. Afzali**[3], **Sydney Bork**[3], **Margaret Campbell**[3], **Taylor Johnson**[1], **Thomas E. Kail**[1], **Richard Martinez**[3], **Tessa Nguyen**[1], **Joseph Sanford**[1,3], **Sara Wist**[3], **Meredith D. Murrell**[4], **Joe M. McCord**[5,6], **Brooks M. Hybertson**[5,6], **Qian Zhang**[1], **Martin A. Javors**[4], **Kelly S. Santangelo**[3], **Karyn L. Hamilton**[1,2]

[1]Department of Health and Exercise Science, Colorado State University, Fort Collins, CO, USA

[2]Columbine Health Systems Center for Healthy Aging, Colorado State University, Fort Collins, CO, USA

[3]Department of Microbiology, Immunology, and Pathology, Colorado State University, Fort Collins, CO, USA

[4]Department of Psychiatry, UT Health San Antonio, TX, USA

[5]Pathways Bioscience, Aurora, CO

[6]Department of Medicine, Division of Pulmonary Sciences and Critical Care Medicine, University of Colorado Anschutz Medical Campus, Aurora, CO

Abstract

Impaired mitochondrial function and disrupted proteostasis contribute to musculoskeletal dysfunction. However, few interventions simultaneously target these two drivers to prevent musculoskeletal decline. Nuclear factor erythroid 2-related factor 2 (Nrf2) activates a transcriptional program promoting cytoprotection, metabolism, and proteostasis. We hypothesized daily treatment with a purported Nrf2 activator, PB125, in Hartley guinea pigs, a model of musculoskeletal decline, would attenuate the progression of skeletal muscle mitochondrial dysfunction and impaired proteostasis and preserve musculoskeletal function. We treated 2-month- and 5-month-old male and female Hartley guinea pigs for 3 and 10 months, respectively, with the phytochemical compound PB125. Longitudinal assessments of voluntary mobility were measured using Any-Maze™ open-field enclosure monitoring. Cumulative skeletal muscle protein synthesis rates were measured using deuterium oxide over the final 30 days of treatment. Mitochondrial

[*]Correspondence: Robert V. Musci, robert.musci@lmu.edu.

Contributions

KSS and KLH conceived of the study and acquired funding. RVM, KMA, KSS, and KLH designed the study. RVM, KMA, MDM, JMM, BMH, MAJ, KSS, and KLH conducted and analyzed PB125 plasma concentration and stability study. RVM, KMA, KSS, KLH supervised acquisition of data from the intervention. RVM, KMA, MAW, ZJV, MAL, MFA, SB, MC, TJ, TEK, RM, TN, JS, SW, KSS, and KLH acquired data, carried out the intervention, managed the animals, and collected tissues. RVM analyzed the data. RVM wrote the original draft of the manuscript. All authors edited, reviewed, and approve of the manuscript.

Competing interests

None.

oxygen consumption in soleus muscles was measured using high resolution respirometry. In both sexes, PB125 1) increased electron transfer system capacity; 2) attenuated the disease/age-related decline in coupled and uncoupled mitochondrial respiration; and 3) attenuated declines in protein synthesis in the myofibrillar, mitochondrial, and cytosolic subfractions of the soleus. These effects were not associated with statistically significant prolonged maintenance of voluntary mobility in guinea pigs. Collectively, treatment with PB125 contributed to maintenance of skeletal muscle mitochondrial respiration and proteostasis in a pre-clinical model of musculoskeletal decline. Further investigation is necessary to determine if these documented effects of PB125 are also accompanied by slowed progression of other aspects of musculoskeletal dysfunction.

Graphical Abstract

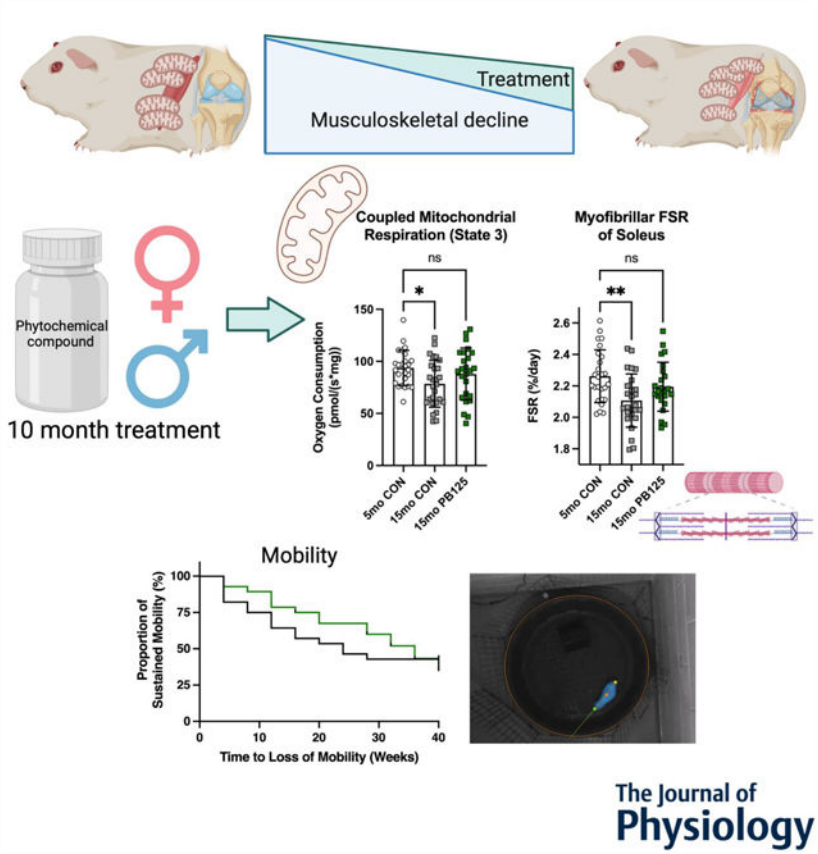

Musculoskeletal decline is an age-related multifactorial syndrome that is characterized by joint degeneration and loss of skeletal muscle function. Mitochondrial dysfunction and impaired protein turnover are two causative factors of musculoskeletal decline. 10 months of daily oral PB125 supplementation attenuated disease-related declines in mitochondrial respiration and protein synthesis in both male and female Hartley guinea pigs, which are a preclinical model of spontaneous and progressive musculoskeletal decline. Despite the attenuation of mitochondrial dysfunction and impaired protein turnover, there was not a statistically significant effect on the maintenance of mobility over the 10-month trial.

Keywords

proteostasis; mitochondria; skeletal muscle; musculoskeletal; chronic disease; ageing; healthspan; lifespan; longevity

Introduction

The musculoskeletal system is comprised of bones, joints, cartilage, tendon, and skeletal muscle, all of which are physically and biochemically connected (Bonewald *et al.*, 2013; DiGirolamo *et al.*, 2013). Age-related decline in musculoskeletal function contributes to the health burden associated with aging (Goates *et al.*, 2019). Moreover, obesity also causes musculoskeletal decline during periods of growth in overweight/obese children and adolescents (Krul *et al.*, 2009; Merder-Coskun *et al.*, 2017) and further drives musculoskeletal dysfunction across the lifespan (Wang *et al.*, 2016). Musculoskeletal dysfunction imparts a loss of mobility and independence (Roux *et al.*, 2005) and leads to frailty (Walston *et al.*, 2006). It also exacerbates comorbidities including cardiometabolic disease (Baskin *et al.*, 2015), cancer (Williams *et al.*, 2018), and cognitive decline (Ogawa *et al.*, 2018); and increases mortality (García-Hermoso *et al.*, 2018). There are no established therapeutics to slow musculoskeletal decline (Yoshimura *et al.*, 2017), including musculoskeletal deficiencies associated with osteoarthritis (OA), which affects over 30 million US adults (US Bone and Joint Initiative, 2020). Accordingly, the NIH identified a critical need (PAR-15-190) to "accelerate the pace of development of novel therapeutics… for preventing and treating key health issues affecting the elderly."

The lack of effective therapeutics for maintaining musculoskeletal function is partially attributable to the insidious nature of musculoskeletal decline in humans, as well as the absence of animal models that recapitulate the multifactorial processes that drive musculoskeletal decline. The Hartley guinea pig is an outbred guinea pig that develops primary (also considered spontaneous or idiopathic) OA that closely resembles disease onset and progression in humans starting at 4 months of age (Jimenez *et al.*, 1997). By nine months of age, these guinea pigs have diminished mobility. At 18 months of age, the severity of OA renders the guinea pigs up to 50% less mobile (Santangelo *et al.*, 2014). Similar to humans with OA (Kemmler *et al.*, 2015; Noehren *et al.*, 2018), skeletal muscle fiber size and density decrease and the proportion of type I fibers increases in the gastrocnemius by 15 months in these guinea pigs (Tonge *et al.*, 2013; Musci *et al.*, 2020). Low skeletal muscle mass in the lower limb is associated with knee osteoarthritis (Lee *et al.*, 2016). Accordingly, the Hartley guinea pig represents a potential model to study musculoskeletal deficiencies associated with OA in a compressed amount of time (i.e. 5 to 15 months of age). Indeed, another lab tested the effect of treatment with metformin and rapamycin, drugs that have beneficial effects on lifespan in mice (Strong *et al.*, 2016), on progression of musculoskeletal dysfunction in Hartley guinea pigs. Surprisingly, the drugs had deleterious effects on OA severity (Minton *et al.*, 2021) and impaired skeletal muscle mitochondrial function (Elliehausen *et al.*, 2021). Thus, there remains a strong need to investigate other therapeutic interventions that can slow the progression of OA and OA-related musculoskeletal dysfunction.

Oxidative stress, mitochondrial dysfunction, and the loss of proteostasis, which are all hallmarks of aging and contribute to other chronic diseases, likely contribute to OA and loss of skeletal muscle function. Cartilage and skeletal muscle are slow to proliferate and have low rates of protein turnover (Vaananen, 1993; Hall, 2012; Relaix *et al.*, 2021) relative to tissues such as liver (Drake *et al.*, 2013). Thus, cartilage and skeletal muscle are susceptible to accumulating oxidative damage and impaired proteome integrity. Targeting mitochondrial dysfunction likely ameliorates not just impaired ATP production and oxidative stress but also other factors that underlie musculoskeletal decline such as impaired proteostasis (protein homeostasis) (Musci *et al.*, 2018). Impaired mitochondrial function is associated with, and precedes, impairments in proteostasis and decrements in skeletal muscle function (Gaffney *et al.*, 2018; Gonzalez-Freire *et al.*, 2018). Inversely, improvements in proteostatic mechanisms regulating mitochondrial proteome integrity would improve mitochondrial function (Hamilton & Miller, 2017), which may in turn alleviate the energetic constraints that impair adequate cellular function. Thus, targeting oxidative stress, mitochondrial function, and/or impaired proteostasis could similarly slow the progression of OA and skeletal muscle decline.

Nuclear factor erythroid 2-related factor 2 (Nrf2) is a transcription factor that regulates hundreds of genes involved in adaptation to stress, including those involved in redox homeostasis, mitochondrial energetics, and proteome maintenance (Gao *et al.*, 2020). Nrf2 activation leads to the upregulation of cytoprotective genes by binding to the antioxidant response element in the promoter regions of target genes, including antioxidant genes such as SOD-1, NQO1, and HO-1 (Katsanos *et al.*, 2006). Nrf2 activation also has anti-inflammatory effects (Ahmed *et al.*, 2017) and has a role in regulating mitochondrial biogenesis (Piantadosi *et al.*, 2008). Transient Nrf2 activation through phytochemical supplementation (Donovan *et al.*, 2012; Reuland *et al.*, 2013; Kubo *et al.*, 2017; Hybertson *et al.*, 2019) is a potential therapeutic intervention that could mitigate chronic diseases (Houghton *et al.*, 2016) and contribute to extended lifespan. Transiently activating Nrf2 targets several interconnected drivers of aging including macromolecular damage, disrupted redox homeostasis (Reuland *et al.*, 2013; Fang *et al.*, 2017), inflammation (Kobayashi *et al.*, 2016), and impaired proteostasis (Konopka *et al.*, 2017). Indeed, treatment with the phytochemical Nrf2 activator Protandim extended median lifespan of male mice in the NIH-NIA Interventions Testing Program (ITP) (Strong *et al.*, 2016).

Given the positive effects of Nrf2 activator treatment, we sought to identify the effects of months-long Nrf2 activator treatment on skeletal muscle mitochondrial respiration and protein turnover in the Hartley guinea pig. Nrf2 activation occurs by a complex set of mechanisms, thus different Nrf2 activators have similar but not identical effects on Nrf2 activity, gene regulation, and physiological endpoints (Baird & Yamamoto, 2020; McCord *et al.*, 2021; Yu & Xiao, 2021). For this study, we utilized the dietary phytochemical combination PB125 as the Nrf2 activator due to the low electrophilic toxicity of its components and potent Nrf2 activating properties (Hybertson *et al.*, 2011; Hybertson *et al.*, 2019; McCord *et al.*, 2021). We hypothesized treatment with Nrf2 activator PB125 would improve skeletal muscle mitochondrial respiration and mechanisms of proteostasis, thereby attenuating musculoskeletal declines in both male and female guinea pigs.

Methods

Husbandry

All procedures were approved by the Colorado State University Institutional Animal Care and Use Committee and were performed in accordance with the NIH Guide for the Care and Use of Laboratory Animals. Dunkin-Hartley guinea pigs were obtained from Charles River Laboratories (Wilmington, MA, USA) at 1- and 4- months of age (mo) for each treatment regimen; 14 male and female guinea pigs were utilized in each age and treatment group (total n = 112) (Figure 1A). As mentioned, Hartley guinea pigs begin developing knee OA at 3 to 5 mo and have severe OA and skeletal muscle and joint phenotypes consistent with aged human musculoskeletal systems by 15 mo (Jimenez *et al.*, 1997; Tonge *et al.*, 2013; Santangelo *et al.*, 2014; Musci *et al.*, 2020). Accordingly, we chose these ages to determine if PB125 could prevent the onset (short term treatment from 2 to 5 mo) or mitigate the progression (long term treatment from 5 to 15 mo) of musculoskeletal dysfunction (Jimenez *et al.*, 1997; Santangelo *et al.*, 2014) and skeletal muscle decline (Musci *et al.*, 2020) (Figure 1A). It is important to note that, because knee OA was progressing as these animals age from 2 to 15 mo, we cannot discern the effect of age itself from disease progression. Additionally, these animals are still experiencing long bone and soft tissue growth until ~10 mo (Watson *et al.*, 1996). Thus, any changes between 5 mo and 15 mo guinea pigs could be a result of disease progression or a maturation/aging process. We acknowledge this is a limitation.

Animals were maintained at Colorado State University's Laboratory Animal Resources housing facilities and were monitored daily by veterinary staff. All guinea pigs were singly-housed in solid bottom cages, maintained on a 12–12 hour light-dark cycle, and provided ad libitum access to food and water. Two control females, two PB125 females, one control male, and two PB125 males required humane euthanasia prior to final analysis due to underlying issues unrelated to treatment (final n = 105). Gross necropsy findings by veterinarians did not raise significant concern as the cause of death in these cases were consistent with what would be expected in conventionally raised guinea pigs.

Measurement of PB125 in OraSweet and in Guinea Pig Plasma using High Performance Liquid Chromatography- Mass Spectrometry (HPLC/MS)

PB125 (Pathways Bioscience, Aurora, CO) is a phytochemical compound comprised of rosemary, ashwagandha, and luteolin powders, which contain the three active ingredients carnosol (CRN), withaferin A (WFA), and luteolin (LUT) at a mixed ratio of 15:5:2 by mass, respectively (Hybertson *et al.*, 2019). Prior to treatment initiation, to ensure adequate compound delivery, plasma levels of each of three primary active ingredients were measured 15, 30, 45, 60, 90, and 120 min post dosing at concentrations of 8, 24, and 48 mg/ml (Figures 1B – 1D), which corresponds with a dosage of 250, 750, and 1250 PPM. The concentration of each drug was reported as μg/ml. Because we prepared weekly allotments of PB125 in OraSweet, we verified the stability of PB125 suspended in OraSweet stored at both room temperature and 4°C for one week (Figure 1E). Compound was kept at 4°C. Reference standards of LUT and WFA were purchased from Sigma Aldrich (St. Louis, MO). CRN was purchased from Cayman Chemical (Ann Arbor, MI). All other reagents were

purchased from Thermo Fisher Scientific (Waltham, MA). HPLC grade methanol was used for preparation of all solutions. Samples were analyzed at the Nathan Shock Core Analytical Pharmacology Core at the University of Texas Health Medical School.

The liquid chromatography tandem mass spectrometry (LC/MS/MS) system consisted of a Shimadzu SIL 20A HT autosampler, LC-20AD pumps (2), and an AB Sciex API 4000 tandem mass spectrometer with turbo ion spray. The LC analytical column was an ACE C8 (50 × 3.0 mm, 3 micron) purchased from Mac-Mod Analytical (Chaddsford, PA). Mobile phase A contained 0.1% formic acid dissolved in water. Mobile phase B contained 0.1% formic acid dissolved in 100% HPLC grade acetonitrile. The LC Gradient was: 0 to 2 min, 25% B; 2 to 6 min, linear gradient to 99% B; 6 to 10 min, 99% B; 10 to 10.01 min, 99% to 25% B min; 10.1 to 12 min, 25%B. LUT and CRN were detected in negative mode using these transitions: 285 to 132.9 m/z and 329 to 285 m/z, respectively. WFA was detected in positive mode at the transition of 471 to 281 m/z.

LUT, CRN, and WFA stock solutions were prepared in methanol at a concentration of 1 mg/ml and stored in aliquots at −80°C. Working stock solutions of each drug were prepared each day from the super stock solutions at a concentration of 100 μg/ml, 10 μg/ml, and 1 μg/ml which were used to spike the calibrators.

Dosages of PB125 in OraSweet were diluted 1000x in 70% ethanol. Calibrator samples were prepared daily by spiking blank OraSweet to achieve final concentrations of 0, 30.4, 152, 760, and 2280 μg/ml. The calibrators were then diluted 1000x in 70% ethanol. The samples were transferred to injection vials and 10 μl was injected into the system. Each drug was quantified by comparing the peak area ratios for each dosage sample against a linear regression of calibrator peak area ratios.

LUT, CRN, and WFA were also quantified in guinea pig plasma. The transitions used were the same as the OraSweet dilutions. Calibrator samples were prepared daily by spiking blank plasma to achieve final concentrations of 0, 5, 10, 25, 50, 100, 500, 1000, and 5000 ng/ml. Calibrators were left to sit for 5 min after spiking. Briefly, 0.1 mL of calibrator and unknown plasma samples were mixed with 1.0 ml of chilled ethanol, vortexed vigorously, and then centrifuged at 17,000 g for 5 min at 25°C. The supernatants were transferred to 1.5 ml microcentrifuge tubes and dried to residue under a nitrogen stream. The residues were then redissolved in 60 μL of 50/50 mobile phase A/mobile phase B and were centrifuged 5 min at 17,000 g. The samples were transferred to injection vials and 15 μL was injected into the LC/MS/MS. Each drug was quantified by comparing the peak area ratios for each unknown sample against a linear regression of calibrator peak area ratios. The concentration of LUT, CRN, and WFA were expressed as ng/mL plasma (Figure 1B – 1D).

Treatment, euthanasia, and tissue acquisition

Based on the analysis conducted at the NSC Analytical Pharmacology Core (Figures 1B – D), we selected a dosage of 8 mg/kg of bodyweight, which corresponds to 250 PPM, about 2.5x the dose of PB125 given to mice in the NIA ITP (https://www.nia.nih.gov/research/dab/interventions-testing-program-itp/compounds-testing) and the lowest dose at which changes in plasma concentration were detected. After a one-month acclimation to

housing conditions, male and female guinea pigs in each age group (2 or 5 months) were randomized to receive a daily oral dose of 8.0 mg/kg bodyweight of PB125 suspended in OraSweet (Perrigo, Dublin, Ireland) or an equivalent volume of OraSweet only (CON). Following established protocol, guinea pigs were given a subcutaneous injection of 0.9% saline enriched with 99% deuterium (^2H_2O) equivalent to 3% of their body weight 30 days prior to euthanasia (Musci *et al.*, 2020). Drinking water was enriched to 8% ^2H_2O for the purpose of maintaining ^2H_2O enrichment of the body water pool during the 30-day labelling period. At the time of harvest, the guinea pigs were 5 mo (after 3 months of treatment) or 15 mo (after 10 months of treatment). In accordance with the standards of the American Veterinary Medical Association, animals were anesthetized with a mixture of isoflurane and oxygen; thoracic cavities were opened and blood was collected via direct cardiac puncture. Whole blood was centrifuged (1200 *g*, 4°C, 15 min) to separate plasma, which was frozen at −80°C until further analysis. After blood collection, the anesthetized animals were transferred a chamber filled with carbon dioxide for euthanasia.

Upon euthanasia, the right soleus of the guinea pig was promptly excised and a portion of the right soleus muscle (~40 mg) was harvested and placed in BIOPS preservation buffer (2.77 mM CaK2-EGTA, 7.23 mM K2-EGTA, 20 mM imidazole, 20 mM taurine, 50 mM K-MES, 0.5 mM dithiothreitol, 6.56 mM MgCl2, 5.77 mM ATP, and 15 mM phosphocreatine, adjusted to pH 7.1) containing 12.5 μM blebbistatin to inhibit muscle contraction (Pesta & Gnaiger, 2011). The rest (~70 mg) of the soleus was frozen in liquid nitrogen and used for other analyses. After excision of the soleus, at least 70 mg of the right gastrocnemius was collected and frozen immediately in liquid nitrogen. Both soleus and gastrocnemius muscles were trimmed of tendons and connective tissue and weighed. Bone marrow was also harvested in saline from the humeri.

Mitochondrial respirometry

After the soleus was placed in BIOPS, the muscle fibers were prepared for high resolution respirometry as follows. Mechanical permeabilization occurred on ice using forceps to separate the fibers. After mechanical permeabilization, fibers underwent chemical permeabilization for 30 min in BIOPS with 12.5 μM blebbistatin and 50 μg/mL saponin, followed by a 15 min rinse in BIOPS. Approximately 2.0 mg (wet weight) of muscle fibers were placed in mitochondrial respiration medium (MiR05, 0.5 mM EGTA, 3 mM $MgCl_2 6H_2O$, 20 mM Taurine, 15 mM Na_2Phosphocreatine, 20 mM Imidazole, 0.5 mM Dithiothreitol, and 50 mM K^+ -MES at pH 7.1) in an Oxygraph-2k (O2K) (Oroboros, Innsbruck, Austria) for high resolution respirometry. To control for oxygen flux at higher concentrations of oxygen, each morning of respirometry analysis, we conducted high oxygen concentration calibrations at 450, 350, 250, and 167 (i.e., concentration of room air) nmol/ml O_2 (Pesta & Gnaiger, 2011). During the experiments, oxygen concentrations were maintained between 225 – 450 nmol/ml O_2. High resolution respirometry measurements were performed in duplicate using two different protocols. Please refer to Table 1 for a detailed explanation of the protocols.

The first protocol (SUIT 1) was an ADP titration protocol to determine ADP sensitivity (Km) and maximal oxidative capacity (Vmax) under Complex I supported respiration. We

measured Complex I supported leak respiration (State $2_{[PGM]}$) with the addition of 10 mM glutamate, 0.5 mM malate, and 5 mM pyruvate. Upon acquisition of State $2_{[PGM]}$, we titrated progressively greater concentrations of ADP from 0.1 mM, 0.175 mM, 0.25 mM, 1 mM, 2 mM, 4 mM, 8 mM, 12 mM, 20 mM, to 24 mM (State $3_{[PGM]}$), awaiting steady-state oxygen flux prior to adding the subsequent titration to determine Complex I linked ADP Vmax and apparent Km (i.e. ADP sensitivity). After the ADP titration was completed, we added 5 mM cytochrome C to test mitochondrial membrane integrity. After cytochrome C addition, we added 10 mM succinate to acquire maximal Complex I and II supported coupled respiration (State $3_{[PGM + S]}$). We then added 0.5 μM FCCP sequentially until there was no increase in respiration to determine the capacity of the electron transport system to consume oxygen, or maximal uncoupled respiration ($ETS_{[CI-CIV]}$). Finally, we added 5 μM rotenone to measure maximal uncoupled respiration with the inhibition of Complex I ($ETS_{[CII-CIV]}$), followed by 2.5 μM Antimycin A to measure residual oxygen consumption (ROX). The respiratory control ratio (RCR: State 3/State 2), which is an index of mitochondrial efficiency was also evaluated.

The second protocol (SUIT 2) measured oxygen consumption while simultaneously measuring ROS production by using the fluorometer attachment of the O2K (Robinson *et al.*, 2019) and addition of 10 μM Amplex Red, 1 U/ml horseradish peroxidase, and 5 U/ml superoxide dismutase. We then measured fatty acid supported leak respiration by adding 10 mM glutamate, 0.5 mM malate, 5 mM pyruvate, and 0.2 mM octanoylcarnitine (State $2_{[PGM + Oct]}$) and 10 mM succinate (State $2_{[PGM + Oct + S]}$). After stimulating maximal leak respiration, we added submaximal boluses of ADP (0.5 mM: (State $3_{[Sub + 0.5D]}$) and 1 mM: State $3_{[Sub + 1.0D]}$), followed by a saturating bolus of ADP (6.0 mM: State $3_{[Sub + 6.0D]}$). We added 5 mM cytochrome C to test mitochondrial membrane integrity. We set a cytochrome C control factor threshold of 0.25. We set this threshold based on the presence of a negative linear relationship between the cytochrome C control factor and State 3 respiration in the SUIT 2 protocol. Upon eliminating respirometry trials that had a cytochrome C control factor of greater than 0.25, the negative linear relationship no longer existed and all samples included in analysis were not biased by over-permeabilization, which is what the cytochrome C control factor approximates (Pesta & Gnaiger, 2011) (Figures 2A – 2C). After the addition of cytochrome C we did not make any further assessments of ROS emission as cytochrome C is a redox substrate. We added 5 μM rotenone to determine maximal coupled respiration in the absence of Complex I (State $3_{[Sub + D - CI]}$) followed by sequential titrations of 0.5 μM FCCP until respiration no longer increased to determine maximal fatty acid supported uncoupled respiration ($ETS_{[Sub + D - CI]}$). and added 2.5 μM antimycin A to measure ROX.

Protein isolation and fractionation

The gastrocnemius and soleus muscles were homogenized and fractionated following established laboratory protocols (Drake *et al.*, 2013; Miller *et al.*, 2013; Groennebaek *et al.*, 2018; Miller *et al.*, 2019; Sieljacks *et al.*, 2019; Musci *et al.*, 2020). Briefly, tissues (20 – 50 mg) were homogenized at 1:10 in isolation buffer (100 mM KCl, 40 mM Tris HCl, 10 mM Tris Base, 5 mM MgCl2, 1 mM EDTA, 1 mM ATP, pH − 7.5) with phosphatase and protease inhibitors (HALT Thermo Scientific, Rockford, IL, USA) using a tissue homogenizer (Bullet

Blender, Next Advance Inc., Averill Park, NY, USA) with zirconium beads (Next Advance Inc., Averill Park, NY, USA). After homogenization, subcellular fractions were isolated via differential centrifugation as previously described (Musci *et al.*, 2020). Once fractionated pellets were isolated and purified, 250 μl 1 M NaOH was added and pellets were incubated for 15 min at 50 °C and 900 RPM.

Sample preparation and analysis via GC/MS: Proteins

Protein subfractions were hydrolyzed in 6 M HCl for 24 hours at 120 °C after which the hydrolysates were ion-exchanged, dried *in vacuo*, and then resuspended in 1 mL of molecular biology grade H_2O. Half of the suspension was derivatized with 500 μL acetonitrile, 50 μL 1 M K_2HPO_4, and 20 μl of pentafluorobenzyl bromide and incubated at 100 °C for 60 min. Derivatives were extracted into ethyl acetate and the organic layer was transferred into vials which were then dried under nitrogen. Samples were reconstituted in ethyl acetate (200 μL – 700 μL).

The derivative of alanine was analyzed on an Agilent 7890A GC coupled to an Agilent 5977A MS as previously described (Robinson *et al.*, 2011; Drake *et al.*, 2013; Miller *et al.*, 2013; Groennebaek *et al.*, 2018; Miller *et al.*, 2019; Sieljacks *et al.*, 2019; Musci *et al.*, 2020). The newly synthesized fraction (f) of proteins was calculated from the true precursor enrichment (p) based upon plasma analyzed for ^2H_2O enrichment and adjusted using mass isotopomer distribution analysis (Busch *et al.*, 2005). Protein synthesis of each subfraction was calculated as the fraction of deuterium-labeled over unlabeled alanine proteins over the entire labeling period (30 days) and expressed as the fractional synthesis rate (FSR). Thus, we divided fraction new by our labeling period (30 days) and multiplied by 100 to express FSR as %/day. Our isotope approach and analysis followed the established procedures detailed in this Core of Reproducibility in Physiology publication (Miller *et al.*, 2020).

Sample preparation and analysis via Gas Chromatography/Mass Spectroscopy (GC/MS): Body water

80 μL of plasma was placed into the inner well of an o-ring cap that was screwed to tube and inverted on a heating block overnight at 100°C. After incubation, 2 μL of 10 M NaOH and 20 μL of acetone were added to the samples and ^2H_2O standards (0 – 20%) and capped immediately, vortexed, and incubated at room temperature overnight. Samples were extracted with 200 μL hexane and the organic layer was transferred through pipette tips filled with anhydrous Na_2SO_4 into GC vials and analyzed via EI mode using a DB-17MS column.

Protein content

Western blotting was used to measure relative content of Nrf2, heme oxygenase (HO-1) and OXPHOS proteins in a subset of tissues. 50–70 mg portions of gastrocnemius and 30 mg portions of soleus (n=9 per treatment group) were powdered under liquid nitrogen and homogenized in a Bullet Blender with zirconium beads and 1.0 mL of radioimmunoprecipitation assay (RIPA) buffer (150 mM NaCl, 0.1 mM EDTA, 50 mM Tris, 0.1% sodium deoxycholate, 0.1% SDS, 1% Triton X-100, pH = 7.50) with HALT protease inhibitors. Samples were reduced (50 μL of B-mercaptoethanol) and heated at 50°C

for 10 min. Approximately 10 μg of protein was loaded into a 4% - 20% Criterion pre-cast gel (Bio-Rad, Hercules, CA, USA) and resolved at 120 V for 120 min. The proteins were then transferred to a PVDF membrane at 100 V for 75 min in transfer buffer (20% w/v methanol, 0.02% w/v SDS, 25 mM Tris Base, 192 mM glycine, pH 8.3). Protein transfer to membrane was confirmed with ponceau stain. Membranes were then blocked and incubated with primary antibodies against Nrf2 (Santa Cruz 13032), HO-1 (Abcam 13243) and total OXPHOS proteins (Abcam 110413) diluted to 1:500, 1:1,000, and 1:500 respectively in 1% milk on a shaker overnight in 4°C. Membranes were rinsed and then incubated with appropriate secondary antibodies (Santa Cruz 2004 (Nrf2 and HO-1) and 2005 (OXPHOS)) diluted to 1:10,000 in 5% BSA for 45 min at room temperature. Protein carbonyls were measured by following the protocol in the commercially available OxiSelect Protein Carbonyl Immunoblot Kit (Cell Biolabs STA-308) as previously performed (Konopka *et al.*, 2015; Konopka *et al.*, 2017). After the membranes were rinsed, SuperSignal West Dura Extended Duration Substrate (Thermo Fisher 34075) was applied and the membranes were subsequently imaged using a FluorChem E Chemiluminescence Imager (Protein Simple, San Diego, CA, USA). Analysis of densitometry was completed using AlphaView SA Software. Units are expressed as density of primary antibody relative to density of ponceau staining.

Mobility

Before the onset of the study, animals were acclimated over a 2-week period to an open circular field behavior monitoring system (ANY-Maze™, Wood Dale, IL) to assess voluntary physical mobility. Animals' activities were recorded, and data were collected for 10 consecutive minutes on a monthly basis throughout the study. Mobility assessments were conducted in the mornings to minimize variance due to time of day. Additionally, cohorts containing both CON and PB125 treated guinea pigs were evaluated on the same day and time. To evaluate the effect of PB125 treatment on the time to event noncompliance, we employed a Kaplan-Meier curve, frequently used to visually summarize time-to-event data (Ranstam & Cook, 2017). The "event" was defined as number of weeks into the study until an animal selected to remain stationary when exposed to the open circular field (i.e., zero distanced traveled in enclosure). Remaining individuals that maintained voluntary mobility throughout the entire 40-week study duration were censored at the 40-week study endpoint.

Statistics

For mitochondrial respirometry, in line with best practices, technical replicates were averaged. The average variability between these technical replicates in this study was 18%, which is standard according to the literature (Jacques *et al.*, 2020). Apparent Km and Vmax values were determined using Michaelis-Menten kinetics in Prism 9.0 (La Jolla, California, USA). For evaluating growth rates, a non-linear Gompertz growth line was fit to the change in body mass over time (i.e. the rate of growth). The rate of growth, k, was compared between treatment and control within in each sex. For respirometry, isotopic measures, and Western blots, three-way ANOVAs were used to measure the main effects of sex, musculoskeletal disease progression/age (referred to as disease/age-related effects from here forward), and PB125 treatment. Post-hoc analyses were performed using Bonferroni's post-hoc test.

To determine the effect of PB125 on disease/age-related changes in mitochondrial respiration and protein synthesis when a significant effect of disease/age was detected, we conducted a subset analysis using a one-way ANOVA with a Dunnett's post-hoc test comparing 15 mo treated and untreated guinea pigs to 5 mo untreated guinea pigs.

Because this study was a secondary project within a larger study with a different primary outcome, we did not design this study to be powered to detect differences in mitochondrial respiration and protein synthesis at a p-value <0.05. Moreover, prior to this study, there was no published data on mitochondrial respiration in permeabilized skeletal muscle fibers of guinea pigs. While we set statistical significance *a priori* at $p<0.05$, we also report differences with $p<0.10$ and corresponding effect sizes to highlight potential directions for future studies.

For measuring sustained mobility, we employed Kaplan-Meier curves combined with log rank and Gehan-Breslow-Wilcoxon tests to assess the probability of sustained voluntary mobility throughout the 10-month study period of the "long term" study.

Data are presented as mean +/− SD. All statistics were performed in Prism 9.0 (La Jolla, California, USA). Cohen's d was calculated by calculating the difference between group means relative to the variance of either group (Sullivan & Feinn, 2012).

Results

Growth rate (k-curves) of the group treated with PB125 did not significantly differ from the control group (CON) as measured by changes of body weight throughout treatment ($p>0.70$ for both sexes) and at euthanasia ($p>0.70$) (Figures 1F – 1H). Moreover, there were no differences in relative skeletal muscle mass between PB125 and CON (Figures 1I & J).

Disease/age-related declines in mitochondrial respiration occur in both male and female guinea pigs

Because mitochondrial respiratory capacity has never been measured in permeabilized skeletal muscle fibers from Hartley guinea pigs, we first evaluated disease/age- and sex-differences in mitochondrial respiration. As a reference, refer to Table 1 for an explanation for each respiratory state mentioned below. Figures 2D – K provide summary titration data. Eleven of 210 trials were excluded due to over-permeabilization (cytochrome C control factor > 0.25; Figures 2A & B). Maximal coupled (State $3_{[CI-CIV]}$) (Figure 3A) and uncoupled (Electron Transport System (ETS) $_{[CI-CIV]}$) (Figure 3B) respiration were significantly greater in males than females (Cohen's d=0.653, 0.735; p=0.006; p=0.002, respectively). Uncoupled Complex II-IV ($ETS_{[CII-CIV]}$) supported respiration was also greater in males (Figure 3C) (Cohen's d=0.668; p=0.002). However, there was no difference in mitochondrial efficiency (RCR) between sexes (Figure 3D) (Cohen's d=0.134, p=0.576). There were no differences in fatty acid supported coupled respiration between sexes at sub-saturating concentrations of ADP (Figures 3E & F) or at saturating (6 mM ADP) concentrations of ADP (Figure 3G) (Cohen's d=0.413; p=0.070).

Disease/age had a negative effect on several aspects of mitochondrial respiration in both male and female guinea pigs. 15 mo male and female guinea pigs had lower coupled (State $3_{[PGM+S]}$) (Figure 3A) and uncoupled ($ETS_{[CI-CIV]}$) (Figure 3B) respiration compared to 5 mo counterparts (Cohen's d=0.731, 0.680; p=0.001, p=0.004, respectively). There was also a disease/age-related decline (Cohen's d=1.388, p<0.0001) in uncoupled respiration without Complex I support ($ETS_{[CII-CIV]}$) (Figure 3C). Disease/age had no effect on fatty acid oxidation supported respiration (Figures 3E – G). Mitochondrial efficiency (RCR) also decreased as a result of disease/age (Cohen's d=0.533, p=0.012) (Figure 3D).

PB125 improves mitochondrial respiration in both male and females

PB125 improved several components of mitochondrial respiration in both 5 mo and 15 mo guinea pigs, and in both males and females. PB125 did not significantly enhance coupled respiration (State 3[PGM+S]) in male and female guinea pigs (Cohen's d=0.357, p=0.098) (Figure 3A), but did significantly increase electron transport system (ETS) capacity ($ETS_{[CI-CIV]}$) (Figure 3B; Cohen's d=0.438, p=0.037). However, PB125 did not influence uncoupled respiration with Complex I inhibited (ETS[CII-CIV]) (Figure 3C; Cohen's d=0.175, p=0.369).

PB125 significantly improved fatty acid supported respiration at sub-saturating (1 mM ADP), but not at saturating (6 mM ADP) concentrations of ADP (Figures 3E & F; Cohen's d=0.519, 0.402, p=0.035, p=0.077, respectively). There was no main effect of PB125 on RCR (Figure 3D; Cohen's d=0.204, p=0.403), a metric of mitochondrial efficiency, or on ROS emission (Figures 3H & I).

PB125 has sex specific effects on mitochondrial ADP kinetics

No O2K data from the ADP titration protocol were excluded based on cytochrome C control factors as all values were below 0.25 (Figure 2A). We determined ADP kinetics by titrating progressively higher concentrations of ADP with saturating amounts of pyruvate, glutamate, and malate. ADP Vmax was greater in both 15 mo male and female guinea pigs compared to 5 mo counterparts (Figure 3J; Cohen's d=0.445, p=0.049). In females, ADP Vmax was lower compared to males (Figure 3J; Cohen's d=0.720, p=0.001). Guinea pigs that received treatment with PB125 had a greater Complex I supported ADP Vmax (Figure 3J; Cohen's d=0.498, p=0.026). Post-hoc comparisons indicate that PB125 improved ADP Vmax in 5 mo female guinea pigs (p=0.045).

Despite ADP Vmax being greater in 15 mo guinea pigs, there was no effect of disease/age on the apparent Km of ADP (Figure 3K). There were also no differences in Km between sexes. However, PB125 did significantly increase the apparent Km (Cohen's d=0.669, p=0.007) indicating lower ADP sensitivity, as there was an increase in ADP Vmax and an absence of change in respiration rates in sub-saturating amounts of ADP (Figures 2D – J). There was a non-significant interaction between sex and PB125 treatment (p=0.092), indicating that the PB125-mediated increase in Km (i.e. decrease in sensitivity) may have occurred only in males.

PB125 attenuates disease/age-related declines in mitochondrial respiration

For any main effects of disease/age on mitochondrial respiration, we evaluated if PB125 attenuated the disease/age-related changes. That is, where we identified significant differences between 5 mo CON and 15 mo CON guinea pigs, but no differences between 5 mo CON and 15 mo PB125 animals, we reported those findings as an attenuating effect of PB125 treatment on age-related changes in mitochondrial respiration. While there was a main positive effect of disease/age on ADP Vmax in the three-way ANOVA (Figure 3J), there was no significant difference in ADP Vmax between 5 mo and 15 mo CON guinea pigs in the subsequent one-way ANOVA analysis (Figure 4A; Cohen's d=0.547, p=0.109). Treated 15 mo guinea pigs, however, had a significantly higher ADP Vmax compared to 5 mo animals (Figure 4A; Cohen's d=0.869, p=0.007). Interestingly, this effect was only observed in males (p=0.021) (Figure 4B). While ADP Vmax was greater in 15 mo guinea pigs, 15 mo guinea pigs had a significantly (Cohen's d=0.709, p=0.024) lower maximal coupled respiration (State $3_{[CI-CIV]}$) compared to 5 mo counterparts (Figure 4C) though this effect was observed in females only (Figure 4D). PB125, however, prevented that disease/age-related decline (Cohen's d=0.270, 0.440, compared to 5 mo CON and 15 mo CON, respectively, Figure 4C). Maximal uncoupled respiration ($ETS_{[CI-CIV]}$) (Figure 4E) was also lower in 15 mo CON compared to 5 mo CON (Cohen's d=0.600), but PB125 prevented the decline (Cohen's d=0.120, 0.480, compared to 5 mo and 15 mo CON, respectively). Further interrogation revealed that 15 mo females had lower $ETS_{[CI-CIV]}$ compared to their 5 mo counterparts, which PB125 attenuated (Figure 4F). Interestingly, when Complex I was inhibited, PB125 had no effect on uncoupled respiration ($ETS_{[CII-CIV]}$) and had no effect on the disease/age-related decline in CII-CIV capacity (Cohen's d=0.202) in either 15 mo males or females (Figures 4G – H). While the RCR of 15 mo CON guinea pigs was lower compared to 5 mo guinea pigs, RCR was not different between 15 mo PB125 treated guinea pigs and 5 mo CON (Figure 4I). However, this occurred only in males where there was a significant difference (p=0.036) between 5 mo and 15 mo CON animals (Figure 4J) but no difference (p=0.151) between 15 mo males treated with PB125 compared to 5 mo CON (Figure 4J). There was no difference in RCR between 5 mo and 15 mo females (Figure 4J). PB125 had no effect on mitochondrial content as assessed by OXPHOS Western blot (data not shown), suggesting that the improvements in mitochondrial respiration are independent of mitochondrial content in skeletal muscle and may reflect improved mitochondrial quality.

Sex- and treatment- and disease/age-related effects on skeletal muscle protein synthesis

To determine whether or not PB125-mediated improvement in mitochondrial respiration was linked to improvements in components of proteostasis, we used ^2H_2O to measure cumulative protein synthesis rates over 30 days. There were no differences in fractional synthesis rate (FSR) in either the gastrocnemius or soleus between male and female guinea pigs (Figure 5). There was a disease/age-related decline in the rates of protein synthesis in all subfractions in the soleus and gastrocnemius of both male and female guinea pigs (p<0.010 for all subfractions) (Figure 5). PB125 did not have a main effect on FSR in any of the subfractions of either muscle from 5 mo or 15 mo, male or female guinea pigs (Figure 5). However, there was a non-significant interaction between age and treatment (p=0.086) in the myofibrillar subfraction of the soleus of both male and female guinea pigs, suggesting that PB125 may have had a positive effect on myofibrillar FSR at 15 mo (Cohen's d=0.533, Figure 5A).

PB125 mitigates disease/age-related declines protein synthesis

Because there was a disease/age-related decline in protein synthesis rates in all subfractions of both the soleus and gastrocnemius, we sought to determine if PB125 prevented any of those declines. PB125 attenuated the disease/age-related decline in myofibrillar FSR of the soleus in both males and females (Figures 6A – B). Additionally, PB125 attenuated the decline in mitochondrial FSR in the soleus (Figure 6C), but these significant differences were no longer detectable when evaluated in males and females separately (Figure 6D). In the soleus, PB125 also mitigated the decline in cytosolic FSR in males only (Figure 6F), but had no effect on the decline in collagen FSR in either sex (Figures 6G & H). In contrast, PB125 had no attenuating effect on the disease/age-related decline in protein synthesis in any subfraction of the gastrocnemius (Figures 6I – P).

The effect of PB125 on downstream Nrf2 targets

To determine how long term PB125 administration affected the Nrf2 pathway, we assessed protein content of Nrf2 and heme oxygenase-1 (HO-1), both of which are downstream targets of Nrf2 activation (Figures 7A & B). There was a disease/age-related increase in Nrf2 protein content (Cohen's d=1.462, p=0.025), but no age-related difference in HO-1 expression. PB125 had a significant effect on Nrf2 protein content (p=0.027), with there being a significant interaction between treatment and disease/age. 5 mo guinea pigs treated with PB125 had greater Nrf2 content compared to CON (Cohen's d=0.832), whereas PB125 treated 15 mo guinea pigs had lower Nrf2 content compared to CON (Cohen's d=1.285). Another target downstream of Nrf2 activation, HO-1 demonstrated a similar disease/age and treatment interaction, particularly in males where 15 mo male guinea pigs had greater HO-1 content compared to 5 mo counterparts (p=0.010). However, PB125 treated 15 mo male guinea pigs had significantly lower protein levels of HO-1 compared to CON counterparts. There was no differences in protein carbonyl content, a marker of protein damage, in the soleus or gastrocnemius (Figures 7C & D).

The effect of PB125 on mobility

To determine whether or not improvements in skeletal muscle mitochondrial respiration and proteostasis translated to improvements in, or maintenance of, mobility, we assessed voluntary activity in an enclosed area using overhead monitoring. We used Kaplan-Meier curves (Figures 7E & F) to depict the probability of sustained voluntary mobility throughout the 40-week study period. There was no statistically significant effect of PB125 on maintained mobility in either male or female guinea pigs. However, CON guinea pigs selected to remain stationary more rapidly than PB125 guinea pigs (Figures 7E & F; grouped sex hazard ratio=0.713, 95% CI=0.3501 to 1.453; median ratio=1.5, CI=0.756 to 2.976; p=0.231). Further, PB125 males tended to have a relative maintenance of mobility compared to controls until about 32 weeks into the study. Interestingly, ~50% of PB125 males were event noncompliant by 36 weeks, while ~50% of CON males maintained mobility the entire 40-week study duration (remaining animals were censored at this time) (Figure 7E). For the majority of the study, PB125 females maintained their mobility compared to CON females. Approximately 50% of control females loss mobility around

16 weeks, while PB125 treated females sustained voluntary mobility until about 28 weeks (Figure 7F).

Discussion

In this study, we tested the effects of a novel phytochemical Nrf2 activator, PB125, on two factors that drive chronic disease in humans: mitochondrial dysfunction and loss of proteostasis in locomotor muscle. PB125 moderately improved various aspects of mitochondrial respiration. We observed that PB125 ameliorated declines in skeletal muscle mitochondrial respiration and protein synthesis in both male and female Hartley guinea pigs, over an age span during which they mature, develop OA, and have increasing mobility impairment. The relatively moderate improvements and maintenance of mitochondrial respiration and proteostatic mechanisms may also be associated with prolonged maintenance of voluntary activity in females. Collectively, this study demonstrates the potential utility of targeting Nrf2 to ameliorate musculoskeletal decline.

Sex- and age/disease-related differences in mitochondrial respiration

This is the first study to measure skeletal muscle mitochondrial respiration in both male and female Hartley guinea pigs using high resolution respirometry. At the time of data collection, there was no mitochondrial respiration data in Hartley guinea pig skeletal muscle. To date, the Konopka group is the only other lab that has published mitochondrial respirometry data in male-only Hartley guinea pig soleus. Following a similar protocol, they found slightly higher (~10–20%) respiration and ADP Vmax values in 8 mo males compared to our 5 mo males (Elliehausen *et al.*, 2021). We sought to characterize differences between male and female guinea pigs at 5 and 15 months of age (mo) to determine sex differences and changes in skeletal muscle mitochondrial respiration as these guinea pigs mature and develop osteoarthritis. We found a clear sex difference in coupled and uncoupled respiration, with females having lower rates of oxygen consumption than males, accompanied by decreased fatty acid supported respiration and ADP kinetics. Interestingly, these differences do not seem to be a consequence of mitochondrial content and may instead reflect intrinsic differences in mitochondrial function. One study in both young and old men and women determined that there was no difference in phosphocreatine recovery post-exercise, a metric of mitochondrial capacity (Kent-Braun & Ng, 2000). However, measuring ATP production using bioluminescence revealed that mitochondria of men have greater capacity to produce ATP than that of women (Karakelides *et al.*, 2010). Employing high resolution respirometry has revealed equivocal results; thus, it remains unclear whether or not females have greater oxidative capacity than males (Cardinale *et al.*, 2018; Miotto *et al.*, 2018). Regardless, it is essential to continue interrogating potential sex differences in mitochondrial function and changes that occur with the progression of osteoarthritis in both sexes.

Mitochondrial function declines with age and contributes to the aging process in humans (Short *et al.*, 2005; Gonzalez-Freire *et al.*, 2015; Distefano *et al.*, 2017; Gonzalez-Freire *et al.*, 2018). However, less is known about changes in mitochondrial function during development in either healthy or overweight adolescents, though obesity seems to lead

to impaired musculoskeletal function in developing adolescents (Krul *et al.*, 2009) and may accelerate the aging process (Salvestrini *et al.*, 2019). We demonstrated that both male and female Hartley guinea pigs experience a decline in mitochondrial respiration as they mature from 5 to 15 mo. Given the relatively young age of these guinea pigs (15 months; ~10% of recorded maximal lifespan (Gorbunova *et al.*, 2008), and ~25% of average companion guinea pig lifespan (Quesenberry *et al.*, 2021)), it is difficult to ascertain if these changes are a consequence of age, the underlying factors that drive OA and musculoskeletal dysfunction, or a combination of both. Other laboratory and companion guinea pigs do not exhibit these musculoskeletal phenotypes as early in their lifespans (Santangelo *et al.*, 2011; Musci *et al.*, 2020). Thus, it is remarkable that despite being relatively young, these guinea pigs demonstrate a decline in mitochondrial respiration. However, this decline could be influenced by a departure from a growth phase (essentially complete by approximately 9 mo in this strain) and/or a consequence of factors that cause or stem from the progression of OA.

Osteoarthritis is associated with impaired mitochondrial respiration and redox regulation in degenerating joints (Loeser, 2010; Collins *et al.*, 2016; Farnaghi *et al.*, 2017; Collins *et al.*, 2018). Interestingly, lower mitochondrial respiration was associated with more severe OA in 9 mo Hartley guinea pigs (Elliehausen et al 2021, Minton et al 2021). In the current study, both coupled and uncoupled respiration, as well as mitochondrial efficiency, declined with age/disease progression in both male and female guinea pig skeletal muscle. There was also a decline in fatty acid supported oxidation. In contrast, ADP Vmax unexpectedly increased with age in both male and female guinea pigs. Given the non-uniform changes in mitochondrial complex protein content (data not shown), it is unlikely differences in mitochondrial content explain the age/disease-related declines in respiration. Moreover, we do not have mitochondrial respiration data in strains of guinea pigs that do not develop OA at these ages. However, these data, as well as other literature, support the notion that impaired mitochondrial respiration is a characteristic of this pre-clinical model of musculoskeletal decline.

PB125 treatment ameliorates disease/age-related declines in mitochondrial respiration

PB125 treated guinea pigs had augmented mitochondrial respiration in 5 mo females and 15 mo males as characterized by greater ADP Vmax and electron transport system capacity $ETS_{[CI-CIV]}$. PB125 did not augment coupled respiration despite improvements in uncoupled respiration, which may reflect enhanced reserve capacity suited to handle greater electron flux. Importantly, PB125 attenuated disease/age-related dysfunction of Complex I and II supported coupled and uncoupled respiration and fatty acid oxidation in both sexes. Notably, PB125 selectively attenuated the disease/age-related decline in coupled respiration in males and uncoupled respiration in females. PB125 attenuated the disease/age-related declines in mitochondrial efficiency/coupling in males only. In humans, mitochondrial coupling decreases with age (Kumaran *et al.*, 2005). Exercise-induced attenuation in loss of mitochondrial efficiency/coupling with age (Conley *et al.*, 2013) has led researchers to speculate that improving mitochondrial efficiency may help attenuate sarcopenia (Harper *et al.*, 2021). Interestingly, in the presence of rotenone, a Complex I inhibitor, there was

no effect of PB125, which suggests that PB125 improves mitochondrial respiration through improvements in Complex I function.

Though PB125 does stimulate Nrf2 activation (as measured by a promoter/reporter assay) *in vitro* (Hybertson et al., 2019), the changes we observed in Nrf2 content with PB125 treatment were not consistent between young and older guinea pigs. Instead, PB125 had a significant interaction with age, increasing Nrf2 content in 5 mo guinea pigs, and decreasing Nrf2 protein expression in 15 mo guinea pigs. HO-1 content showed a similar pattern. Though we have no acute in vivo data to support this, we hypothesize that PB125 activated Nrf2, as demonstrated by greater Nrf2 content in 5 mo guinea pigs. 10 months of treatment with PB125 led to consistent Nrf2 activation, leading to greater downstream antioxidant enzymes. With age, we hypothesize that greater basal levels of ROS led to a greater Nrf2 content in 15 mo CON guinea pig. We further posit that PB125 ameliorated the increase in age-related ROS, which led to significantly lower levels of Nrf2 and HO-1. This pattern is similar to aerobic exercise, which upregulates antioxidative capacity and protects from age-related increases in oxidative stress (Muthusamy *et al.*, 2012). In humans, Nrf2 expression increases with age; however, aerobic exercise training reduces levels of Nrf2 (Ostrom & Traustadottir, 2020). We speculate a similar pattern occurred with PB125 treatment, though further work is required to understand how PB125 affects Nrf2 activation in vivo in both young and old organisms. Similar to many drugs and supplements, it is quite possible that PB125 has widespread effects that are not mediated through a singular pathway.

A different Nrf2 activator, sulforaphane, similarly improved Complex I function (Bose *et al.*, 2020) as PB125 had in the present study. The pathways underlying the effect of Nrf2 activation on mitochondrial respiration are not entirely understood. Several studies have demonstrated that Nrf2 is a central mediator for exercise-induced mitochondrial biogenesis and improvements in mitochondrial function (Merry & Ristow, 2016; D'Souza *et al.*, 2020; Islam *et al.*, 2020). Interestingly, both Nrf2-related redox signaling (Safdar *et al.*, 2010) and Complex I function decrease with age in skeletal muscle (Kruse *et al.*, 2016). Thus, PB125 may target a critical mechanism that contributes to mitochondrial dysfunction, though the specific mechanisms by which Nrf2 activation might contribute to Complex I function remain to be elucidated.

As a master regulator of cytoprotective gene transcription, Nrf2 is a critical component of redox homeostasis. Skeletal muscle mitochondria of aged Nrf2 knock-out mice emit significantly more ROS than aged wildtype counterparts reflecting the role of Nrf2 in regulating redox balance (Kitaoka *et al.*, 2019). *In vitro*, Nrf2 knock out models have compromised Complex I activity due to impairments in NADH availability (Kovac *et al.*, 2015). Importantly, pyruvate dehydrogenase is a redox sensitive enzyme responsible for supplying NADH to Complex I (Fisher-Wellman *et al.*, 2015). Thus, age-related increases in oxidative stress may constrain the supply of NADH to Complex I, which would explain age-associated decline in Complex I capacity and how NAD+ supplementation restores mitochondrial respiratory capacity (Kruse *et al.*, 2016; McElroy *et al.*, 2020). In our study, PB125 increased mitochondrial respiration, particularly in Complex I, which may have been mediated by improved cellular redox regulation. However, future studies will need to more rigorously investigate the effect of PB125 on redox homeostasis.

Another potential mechanism by which PB125 enhanced mitochondrial respiration in this study is through greater mitochondrial protein turnover. However, there was a decline in mitochondrial biogenesis as these guinea pigs matured and OA developed, suggesting that, in order to maintain mitochondrial density, degradation of mitochondrial proteins (i.e. mitophagy or ubiquitin dependent degradation of mitochondrial proteins) also declined. Impaired mitophagy contributes to mitochondrial dysfunction and disease in humans (Ryu *et al.*, 2016; Gouspillou *et al.*, 2018; Newman & Shadel, 2018). Importantly, PB125 attenuated the age/disease-related decline in mitochondrial protein synthesis, suggesting that declines in degradation/mitophagy may have also been attenuated, though we did not directly measure this. As such, we posit that mitochondrial protein turnover, which is essential for maintenance of overall mitochondrial function (Szczepanowska & Trifunovic, 2021), was maintained in 15 mo PB125 guinea pigs compared to 15 mo CON guinea pigs in this study. Others have also demonstrated that Nrf2 activators play a role in modulating mitochondrial protein turnover. In *C. elegans* the Nrf2 homolog mediated Tomatidine-induced (a Nrf2 activator) mitophagy (Fang *et al.*, 2017). Our group has demonstrated that Protandim, also a phytochemical Nrf2 activator, enhanced mitochondrial protein turnover in wheel running rats (Bruns *et al.*, 2018). Thus, Nrf2 activation seems to preserve mitochondrial protein turnover in 15 mo guinea pigs while turnover may have declined in 15 mo CON guinea pigs. Interestingly, the Konopka group published mitochondrial respiration data in Hartley guinea pigs treated with either rapamycin or rapamycin combined with metformin, interventions reported to have anti-aging effects, following similar mitochondrial respiration protocols as the present study. Surprisingly, they reported that both rapamycin and rapamycin combined with metformin had deleterious effects on mitochondrial respiration (Elliehausen *et al.*, 2021) and worsened OA severity (Minton *et al.*, 2021). In contrast, the PB125-induced improvements in the present study also led to ameliorating OA severity in the same guinea pigs (*In preparation*). Altogether, these data support that PB125 can attenuate age related declines in mitochondrial respiration, which may in turn lead to the maintenance of musculoskeletal health.

PB125 attenuates declines in components of protein homeostasis

Decline in mechanisms to maintain proteostasis (which include not only protein synthesis and degradation, but also chaperone-mediated folding and protein trafficking (Noack *et al.*, 2014)) contributes to musculoskeletal dysfunction (Kaushik & Cuervo, 2015; Santra *et al.*, 2019). There is limited insight on the effect of either age or OA progression on protein homeostasis in humans, though basal protein synthesis appears to be unchanged with age in humans (Volpi *et al.*, 2001; Brook *et al.*, 2016). Moreover, it is unclear whether or not both men and women experience a decline in proteostasis with age. While men generally have greater muscle mass than women, men also lose muscle mass faster and muscle strength to a greater degree; however, women are less fatigue resistant (thoroughly reviewed in (Gheller *et al.*, 2016). In the present study, we documented declines in protein synthesis in all subfractions of the soleus and gastrocnemius muscles of both male and female Hartley guinea pigs. There were no sex differences in fractional synthesis rates in either muscle. This is the first study to characterize declines in protein synthesis in female Hartley guinea pigs. However, these declines could be attributed to the fact that we compared skeletal muscle protein synthesis rates of 5 mo guinea pigs, while they are still growing, to 15 mo

guinea pigs, which have plateaued in body weight (Figures 2A & 2B). We have previously documented that rates of skeletal muscle protein synthesis in 15 mo male Hartley guinea pigs are slower than 9 mo Hartley guinea pigs, which is the age at which growth plateaus (Figures 1F & G) (Musci *et al.*, 2020). Thus, the decline in protein synthesis observed in the present study may be a consequence of both reaching maturity as well as musculoskeletal decline consistent with either musculoskeletal disease progression or advancing age.

We documented differences in long-term protein synthesis rates to minimize the bias of faster turning over proteins (Miller *et al.*, 2015); however, it is possible that our approach may still not identify differences in fractional synthesis rates between ages if the protein pools subject to turnover (i.e. the dynamic protein pools) are not the same between the 5 mo and 15 mo guinea pigs. As recently demonstrated by Abbott and colleagues, the dynamic protein pool declines with age and, thus, can obscure the fractional synthesis rates and biases towards aged animals having lower synthesis rates (Abbott *et al.*, 2021). The approach the authors utilized raises important considerations for evaluating the effect of age or interventions on protein turnover in future studies. Employing such an approach may also help reconcile differences in observations on the effect of age on protein turnover between species (Volpi *et al.*, 2001; Miller *et al.*, 2019; Musci *et al.*, 2020) and more accurately describe the age-related effects on protein kinetics.

The mechanisms by which PB125 attenuated the decline in protein synthesis are not entirely clear. It is worth noting that the attenuation in protein synthesis occurred only in the soleus. It is unclear why there is a muscle-specific effect. However, the soleus muscle is primarily comprised of type I myofibers and gastrocnemius is much more mixed (Musci *et al.*, 2020). PB125-mediated improvements in mitochondrial respiration likely alleviated energetic constraints. Protein turnover is energetically demanding, accounting for nearly 35% of basal metabolism (Waterlow, 1984; Rolfe & Brown, 1997; Bier, 1999). Impairments in mitochondrial function consequentially constrain the amount of energy dedicated to proteostasis. Mitochondrial dysfunction precedes the loss of proteostasis in skeletal muscle, which leads to declines in function (Ben-Zvi *et al.*, 2009; Gaffney *et al.*, 2018). Moreover, other interventions that attenuate the decline in or improve mitochondrial function, also improve proteostatic mechanisms and preserve overall muscle function. For example, maintaining physical activity and caloric restriction in rodents delays declines in mitochondrial respiration as well as skeletal muscle function (Zangarelli *et al.*, 2006; Stolle *et al.*, 2018), a similar observation made in masters athletes (Zampieri *et al.*, 2015). While both exercise and caloric restriction have broad effects, more targeted interventions focused on improving mitochondrial function also report a similar phenomenon: enhancing mitochondrial function delays skeletal muscle dysfunction (Gaffney *et al.*, 2018; Campbell *et al.*, 2019). This observation occurs in other tissues as well. Increasing mitochondrial proteostasis decreases proteotoxic amyloid aggregation in cells, increasing fitness and lifespan in *C. elegans* (Sorrentino et al., 2017). These studies emphasize the importance of mitochondrial respiration and the production of ATP to facilitate proteostatic mechanisms. In humans, aerobic exercise improves mitochondrial function through mitochondrial remodeling and improves skeletal muscle function (Greggio *et al.*, 2017). Altogether, our data support the posit that PB125-mediated improvements in mitochondrial respiration

alleviated constraints in energy which led to greater amount of ATP available to support proteostasis.

Another mechanism by which PB125 may have attenuated declines in skeletal muscle proteostasis is through the mitigation of inflammation and oxidative stress, which can have deleterious effects on protein turnover, particularly protein synthesis. Protein synthesis, at rest, appears to be no different between young and old individuals (Volpi *et al.*, 2001; Brook *et al.*, 2016). However, age-related inflammation and oxidative stress can blunt the anabolic response to stimuli such as exercise or feeding. This concept, termed anabolic resistance, is a contributor to age-related musculoskeletal dysfunction and appears to blunt the anabolic response to resistance exercise training (Cuthbertson *et al.*, 2005; Wilkes *et al.*, 2009; Brook *et al.*, 2016). Interventions designed to mitigate age-related increases in oxidative stress or inflammation seem to improve skeletal muscle anabolic responses to exercise (Trappe *et al.*, 2002), feeding (Rieu *et al.*, 2009; Smiles *et al.*, 2019), and insulin (Rivas *et al.*, 2016). There is an increase in some systemic inflammatory mediators in these Hartley guinea pigs, which may be associated with OA (Huebner *et al.*, 2007; Santangelo *et al.*, 2011). Importantly, PB125 stimulates transcription of endogenous antioxidant and anti-inflammatory genes (Hybertson *et al.*, 2011; Hybertson *et al.*, 2019). Thus, it is possible that PB125 treatment ameliorated oxidative stress and inflammation and improved the anabolic response to feeding. However, because we measured cumulative protein synthesis over 30 days, rather than acutely in response to an anabolic stimulus such as feeding, we cannot determine if there were any changes specifically in the anabolic response to feeding. Future studies should investigate the efficacy of PB125 on abrogating inflammation and oxidative stress and, in acute settings, determine whether targeting Nrf2 could enhance the anabolic response to feeding or activity. In the present study, there was no observed effect of treatment on ROS emission or protein oxidation. However, our lab has previously demonstrated that another Nrf2 activator increases antioxidant protein expression (Reuland *et al.*, 2013) and augmented protein synthesis related to proteostasis in skeletal muscle of rats in response to wheel running exercise (Bruns *et al.*, 2018). Thus, treatment with Nrf2 activators may represent a class of interventions that augment adaptation to acute stressors (Musci *et al.*, 2019).

Future Directions

The improvements in mitochondrial respiration and proteostasis did not translate to statistically significant improvements in sustained mobility. However, it is important to note that our measure of mobility is only one metric of musculoskeletal function. Additionally, musculoskeletal function is not the only factor that dictates mobility. For example, we recently demonstrated that these guinea pigs exhibit hallmarks of human Alzheimer's disease that could explain impairments in integrative functional outcomes such as gait (Wahl *et al.*, 2022). Thus, it is still important to assess additional and more specific components of musculoskeletal function, as mitochondrial function is a strong determinant in physical function such as gait speed and grip strength in humans (Gonzalez-Freire *et al.*, 2018).

Another observation that warrants further investigation are the sex-specific effects of PB125. Other interventions involving Nrf2 activators have also demonstrated sex-specific effects.

The Interventions Testing Program reported that treatment with the Nrf2 activator Protandim extended median lifespan in heterogenous male mice, but not females (Strong *et al.*, 2016). Our lab has also previously demonstrated that Protandim only improved myofibrillar proteostasis in men (Konopka *et al.*, 2017). Other healthspan promoting interventions, such as a metformin and rapamycin, also have sex specific effects (Strong *et al.*, 2016). We have begun interrogating these sex specific effects through the use of kinetic proteomics (Wolff *et al.*, 2019; Wolff *et al.*, 2021). Moving forward, it will be necessary to interrogate the sex differences in the present study and the implications they have on the efficacy of PB125 to attenuate musculoskeletal decline in men and women, as they experience similar prevalence worldwide (Shafiee *et al.*, 2017).

A limitation of the study was comparing guinea pigs still in the growth/maturation process to those that have finished growing. While Hartley guinea pigs reach sexual maturity by 4 mo, our data demonstrate they do not cease growing until 9 mo. Nonetheless, even at a relatively young age, these Hartley guinea pigs are an established model of age-related knee osteoarthritis (Jimenez *et al.*, 1997; Santangelo *et al.*, 2014). Thus, some of the comparisons made could be a consequence of comparing guinea pigs that are growing to those that are not. Regardless, the phenotype exhibited by these guinea pigs still reflects age-related OA and musculoskeletal decline in humans. The aim of our study was to determine whether long term supplementation of a phytochemical compound could ameliorate the progression of age-related OA- and musculoskeletal decline documented in this model (Musci *et al.*, 2020; Elliehausen *et al.*, 2021; Minton *et al.*, 2021). Further, our group has also documented that brains of these guinea pigs exhibit hallmarks of human brain aging (Wahl *et al.*, 2022). Future studies should focus on comparisons in these guinea pigs after the growth phase. Such studies would reveal how the musculoskeletal system changes after maturation and while OA continues to progress, as well as provide opportunities to test potential interventions that target both aging and musculoskeletal dysfunction. However, a significant barrier to asking such questions is that OA is often so severe in Hartley guinea pigs at 18 mo, that veterinarians often recommend euthanasia. However, future studies could study interventions between from 10 mo to 18 mo, after the growth phase has completed.

The decline in mitochondrial respiration while these guinea pigs were still maturing also raises interesting future directions, particularly in trying to determine how mitochondrial function may play a role in adequate organismal development. Another direction is to further interrogate the decline in mitochondrial function and protein synthesis during active growth. Of note, Hartley guinea pigs experience an increase in systemic inflammation during development and OA progression (Santangelo *et al.*, 2011) and experience an increase in adiposity (Radakovich *et al.*, 2019; Musci *et al.*, 2020). Accordingly, it is tempting to suggest these Hartley guinea pigs may represent a model for adolescent obesity. However, additional studies are necessary comparing the development of Hartley guinea pigs to a strain of guinea pigs not as susceptible to inflammation and OA during development (i.e. up to 12 mo).

Conclusions

Musculoskeletal dysfunction is a primary contributor to disability and loss of independence in humans. There are few existing interventions that effectively mitigate the decline in skeletal muscle function, particularly in aging individuals and/or adolescents and younger adults with OA. In this study, we further characterized a model of musculoskeletal dysfunction measuring mitochondrial respiration and protein synthesis in both male and female Hartley guinea pigs. Moreover, we tested a potential healthspan-extending phytochemical compound PB125, which is currently in the NIA-ITP (https://www.nia.nih.gov/research/dab/interventions-testing-program-itp/compounds-testing), on mitochondrial respiration and proteostasis in this pre-clinical guinea pig model of musculoskeletal decline. We found that PB125 improved mitochondrial respiration and attenuated declines in protein synthesis, mechanisms that could contribute to improvements in function and longevity. This project adds to the growing literature that supports the use of Nrf2 activators to improve organismal health. The data from this study provide mechanistic insight by which a readily translatable intervention could mitigate musculoskeletal decline in humans.

Supplementary Material

Refer to Web version on PubMed Central for supplementary material.

Acknowledgments

We would like to thank Dr. Benjamin Miller of the Aging & Metabolism Research Program of the Oklahoma Medical Research Foundation for his insightful critiques and assistance in study design and data interpretation. The authors also acknowledge Dr. Ann Hess of the Statistics Department at Colorado State University for overseeing and guiding the statistical analysis of this project. We would also like to thank Dr. Dan Lark of the Health and Exercise Department at Colorado State University for providing guidance in assessing and analyzing mitochondrial respirometry data. Ted Bowers and Will Mahoney assisted with skeletal muscle tissue processing. Pathways Bioscience provided the PB125 compound for this project.

Funding

This work was funded by NIH grant R21 AG054713–02 awarded to KLH and KSS and supported by the ACSM NASA Space Physiology Grant 18-00843 awarded to RVM.

Biography

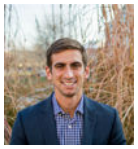

Robert Musci is an Assistant Professor in the Health and Human Sciences Department of Loyola Marymount University. He earned his doctorate in Human Bioenergetics at Colorado State University in the Translational Research on Aging and Chronic Disease Lab and subsequently worked as a postdoctoral research fellow in the Kardon Lab at the University of Utah. His research now involves investigating mechanisms to improve the healthspan by translating basic and preclinical research into human interventions.

Data Availability Statement

All supporting data can be found in the paper. Additional original data and/or Western blot images can be provided upon request. Contact RVM and KLH describing the specific data requested and the intended use of the data.

References

Abbott CB, Lawrence MM, Kobak KA, Lopes EBP, Peelor FF 3rd, Donald EJ, Van Remmen H, Griffin TM & Miller BF. (2021). A Novel Stable Isotope Approach Demonstrates Surprising Degree of Age-Related Decline in Skeletal Muscle Collagen Proteostasis. Function (Oxf) 2, zqab028. [PubMed: 34124684]

Ahmed SM, Luo L, Namani A, Wang XJ & Tang X. (2017). Nrf2 signaling pathway: Pivotal roles in inflammation. Biochim Biophys Acta Mol Basis Dis 1863, 585–597. [PubMed: 27825853]

Baird L & Yamamoto M. (2020). The Molecular Mechanisms Regulating the KEAP1-NRF2 Pathway. Mol Cell Biol 40, e00099–00020. [PubMed: 32284348]

Baskin KK, Winders BR & Olson EN. (2015). Muscle as a “mediator” of systemic metabolism. Cell Metab 21, 237–248. [PubMed: 25651178]

Ben-Zvi A, Miller EA & Morimoto RI. (2009). Collapse of proteostasis represents an early molecular event in Caenorhabditis elegans aging. Proc Natl Acad Sci U S A 106, 14914–14919. [PubMed: 19706382]

Bier DM. (1999). The Role of Protein and Amino Acids in Sustaining and Enhancing Performance. National Academies Press.

Bonewald LF, Kiel DP, Clemens TL, Esser K, Orwoll ES, O’Keefe RJ & Fielding RA. (2013). Forum on bone and skeletal muscle interactions: summary of the proceedings of an ASBMR workshop. J Bone Miner Res 28, 1857–1865. [PubMed: 23671010]

Bose C, Alves I, Singh P, Palade PT, Carvalho E, Børsheim E, Jun S-R, Cheema A, Boerma M, Awasthi S & Singh SP. (2020). Sulforaphane prevents age-associated cardiac and muscular dysfunction through Nrf2 signaling. Aging Cell, e13261. [PubMed: 33067900]

Brook MS, Wilkinson DJ, Mitchell WK, Lund JN, Phillips BE, Szewczyk NJ, Greenhaff PL, Smith K & Atherton PJ. (2016). Synchronous deficits in cumulative muscle protein synthesis and ribosomal biogenesis underlie age-related anabolic resistance to exercise in humans. J Physiol 594, 7399–7417. [PubMed: 27654940]

Bruns DR, Ehrlicher SE, Khademi S, Biela LM, Peelor FF 3rd, Miller BF & Hamilton KL. (2018). Differential effects of vitamin C or protandim on skeletal muscle adaptation to exercise. J Appl Physiol (1985) 125, 661–671. [PubMed: 29856263]

Busch R, Kim Y-K, Neese RA, Schade-Serin V, Collins M, Awada M, Gardner JL, Beysen C, Marino ME, Misell LM & Hellerstein MK. (2005). Measurement of protein turnover rates by heavy water labeling of nonessential amino acids. Biochimica Et Biophysica Acta Bba - Gen Subj 1760, 730–744.

Busch R, Neese RA, Awada M, Hayes GM & Hellerstein MK. (2007). Measurement of cell proliferation by heavy water labeling. Nat Protoc 2, 3045–3057. [PubMed: 18079703]

Campbell MD, Duan J, Samuelson AT, Gaffrey MJ, Merrihew GE, Egertson JD, Wang L, Bammler TK, Moore RJ, White CC, Kavanagh TJ, Voss JG, Szeto HH, Rabinovitch PS, MacCoss MJ, Qian WJ & Marcinek DJ. (2019). Improving mitochondrial function with SS-31 reverses age-related redox stress and improves exercise tolerance in aged mice. Free Radic Biol Med 134, 268–281. [PubMed: 30597195]

Cardinale DA, Larsen FJ, Schiffer TA, Morales-Alamo D, Ekblom B, Calbet JAL, Holmberg HC & Boushel R. (2018). Superior Intrinsic Mitochondrial Respiration in Women Than in Men. Front Physiol 9, 1133. [PubMed: 30174617]

Collins JA, Diekman BO & Loeser RF. (2018). Targeting aging for disease modification in osteoarthritis. Curr Opin Rheumatol 30, 101–107. [PubMed: 28957964]

Collins JA, Wood ST, Nelson KJ, Rowe MA, Carlson CS, Chubinskaya S, Poole LB, Furdui CM & Loeser RF. (2016). Oxidative Stress Promotes Peroxiredoxin Hyperoxidation and Attenuates Pro-survival Signaling in Aging Chondrocytes. J Biol Chem 291, 6641–6654. [PubMed: 26797130]

Conley KE, Jubrias SA, Cress ME & Esselman PC. (2013). Elevated energy coupling and aerobic capacity improves exercise performance in endurance-trained elderly subjects. Exp Physiol 98, 899–907. [PubMed: 23204291]

Cuthbertson D, Smith K, Babraj J, Leese G, Waddell T, Atherton P, Wackerhage H, Taylor PM & Rennie MJ. (2005). Anabolic signaling deficits underlie amino acid resistance of wasting, aging muscle. Faseb J 19, 422–424. [PubMed: 15596483]

D'Souza RF, Woodhead JST, Hedges CP, Zeng NN, Wan JX, Kumagai H, Lee C, Cohen P, Cameron-Smith D, Mitchell CJ & Merry TL. (2020). Increased expression of the mitochondrial derived peptide, MOTS-c, in skeletal muscle of healthy aging men is associated with myofiber composition. Aging-Us 12, 5244–5258.

DiGirolamo DJ, Kiel DP & Esser KA. (2013). Bone and skeletal muscle: neighbors with close ties. J Bone Miner Res 28, 1509–1518. [PubMed: 23630111]

Distefano G, Standley RA, Dube JJ, Carnero EA, Ritov VB, Stefanovic-Racic M, Toledo FG, Piva SR, Goodpaster BH & Coen PM. (2017). Chronological Age Does not Influence Ex-vivo Mitochondrial Respiration and Quality Control in Skeletal Muscle. J Gerontol A Biol Sci Med Sci 72, 535–542. [PubMed: 27325231]

Donovan EL, McCord JM, Reuland DJ, Miller BF & Hamilton KL. (2012). Phytochemical activation of Nrf2 protects human coronary artery endothelial cells against an oxidative challenge. Oxid Med Cell Longev 2012, 132931. [PubMed: 22685617]

Drake JC, Bruns DR, Peelor FF 3rd, Biela LM, Miller RA, Hamilton KL & Miller BF. (2014). Long-lived crowded-litter mice have an age-dependent increase in protein synthesis to DNA synthesis ratio and mTORC1 substrate phosphorylation. Am J Physiol Endocrinol Metab 307, E813–821. [PubMed: 25205819]

Drake JC, Bruns DR, Peelor FF 3rd, Biela LM, Miller RA, Miller BF & Hamilton KL. (2015). Long-lived Snell dwarf mice display increased proteostatic mechanisms that are not dependent on decreased mTORC1 activity. Aging Cell 14, 474–482. [PubMed: 25720574]

Drake JC, Peelor FF 3rd, Biela LM, Watkins MK, Miller RA, Hamilton KL & Miller BF. (2013). Assessment of mitochondrial biogenesis and mTORC1 signaling during chronic rapamycin feeding in male and female mice. J Gerontol A Biol Sci Med Sci 68, 1493–1501. [PubMed: 23657975]

Elliehausen CJ, Minton DM, Nichol AD & Konopka AR. (2021). Skeletal muscle mitochondrial respiration in a model of age-related osteoarthrtiis is impaired after dietary rapamycin. bioRxiv.

Fang EF, Waltz TB, Kassahun H, Lu QP, Kerr JS, Morevati M, Fivenson EM, Wollman BN, Marosi K, Wilson MA, Iser WB, Eckley DM, Zhang YQ, Lehrmann E, Goldberg IG, Scheibye-Knudsen M, Mattson MP, Nilsen H, Bohr VA & Becker KG. (2017). Tomatidine enhances lifespan and healthspan in C-elegans through mitophagy induction via the SKN-1/Nrf2 pathway. Scientific Reports 7, 46208. [PubMed: 28397803]

Farnaghi S, Prasadam I, Cai G, Friis T, Du Z, Crawford R, Mao X & Xiao Y. (2017). Protective effects of mitochondria-targeted antioxidants and statins on cholesterolinduced osteoarthritis. Faseb J 31, 356–367. [PubMed: 27737897]

Fisher-Wellman KH, Lin CT, Ryan TE, Reese LR, Gilliam LA, Cathey BL, Lark DS, Smith CD, Muoio DM & Neufer PD. (2015). Pyruvate dehydrogenase complex and nicotinamide nucleotide transhydrogenase constitute an energy-consuming redox circuit. Biochem J 467, 271–280. [PubMed: 25643703]

Gaffney CJ, Pollard A, Barratt TF, Constantin-Teodosiu D, Greenhaff PL & Szewczyk NJ. (2018). Greater loss of mitochondrial function with ageing is associated with earlier onset of sarcopenia in C. elegans. Aging 10, 1 15. [PubMed: 29348393]

Gao L, Kumar V, Vellichirammal NN, Park SY, Rudebush TL, Yu L, Son WM, Pekas EJ, Wafi AM, Hong J, Xiao P, Guda C, Wang HJ, Schultz HD & Zucker IH. (2020). Functional, proteomic and bioinformatic analyses of Nrf2- and Keap1- null skeletal muscle. J Physiol 598, 5427–5451. [PubMed: 32893883]

García-Hermoso A, Cavero-Redondo I, Ramírez-Vélez R, Ruiz J, Ortega FB, Lee D-C & Martínez-Vizcaíno V. (2018). Muscular strength as a predictor of all-cause mortality in apparently healthy population: a systematic review and meta-analysis of data from approximately 2 million men and women. Arch Phys Med Rehab 99, 2100–2113.e2105.

Gheller BJ, Riddle ES, Lem MR & Thalacker-Mercer AE. (2016). Understanding Age-Related Changes in Skeletal Muscle Metabolism: Differences Between Females and Males. Annu Rev Nutr 36, 129–156. [PubMed: 27431365]

Goates S, Du K, Arensberg MB, Gaillard T, Guralnik J & Pereira SL. (2019). Economic Impact of Hospitalizations in US Adults with Sarcopenia. J Frailty Aging 8, 93–99. [PubMed: 30997923]

Gonzalez-Freire M, de Cabo R, Bernier M, Sollott SJ, Fabbri E, Navas P & Ferrucci L. (2015). Reconsidering the Role of Mitochondria in Aging. J Gerontol A Biol Sci Med Sci 70, 1334–1342. [PubMed: 25995290]

Gonzalez-Freire M, Scalzo P, D'Agostino J, Moore ZA, Diaz-Ruiz A, Fabbri E, Zane A, Chen B, Becker KG, Lehrmann E, Zukley L, Chia CW, Tanaka T, Coen PM, Bernier M, de Cabo R & Ferrucci L. (2018). Skeletal muscle ex vivo mitochondrial respiration parallels decline in vivo oxidative capacity, cardiorespiratory fitness, and muscle strength: The Baltimore Longitudinal Study of Aging. Aging Cell 17.

Gorbunova V, Bozzella MJ & Seluanov A. (2008). Rodents for comparative aging studies: from mice to beavers. Age (Dordr) 30, 111–119. [PubMed: 19424861]

Gouspillou G, Godin R, Piquereau J, Picard M, Mofarrahi M, Mathew J, Purves-Smith FM, Sgarioto N, Hepple RT, Burelle Y & Hussain SNA. (2018). Protective role of Parkin in skeletal muscle contractile and mitochondrial function. J Physiol 596, 2565–2579. [PubMed: 29682760]

Greggio C, Jha P, Kulkarni SS, Lagarrigue S, Broskey NT, Boutant M, Wang X, Conde Alonso S, Ofori E, Auwerx J, Canto C & Amati F. (2017). Enhanced Respiratory Chain Supercomplex Formation in Response to Exercise in Human Skeletal Muscle. Cell Metab 25, 301–311. [PubMed: 27916530]

Groennebaek T, Jespersen NR, Jakobsgaard JE, Sieljacks P, Wang J, Rindom E, Musci RV, Botker HE, Hamilton KL, Miller BF, de Paoli FV & Vissing K. (2018). Skeletal Muscle Mitochondrial Protein Synthesis and Respiration Increase With Low-Load Blood Flow Restricted as Well as High-Load Resistance Training. Front Physiol 9, 1796. [PubMed: 30618808]

Hall BK. (2012). Cartilage V1: Structure, Function, and Biochemistry. Elsevier Science.

Hamilton KL & Miller BF. (2017). Mitochondrial proteostasis as a shared characteristic of slowed aging: the importance of considering cell proliferation. J Physiol 595, 6401–6407. [PubMed: 28719097]

Harper C, Gopalan V & Goh J. (2021). Exercise rescues mitochondrial coupling in aged skeletal muscle: a comparison of different modalities in preventing sarcopenia. J Transl Med 19, 71. [PubMed: 33593349]

Houghton CA, Fassett RG & Coombes JS. (2016). Sulforaphane and Other Nutrigenomic Nrf2 Activators: Can the Clinician's Expectation Be Matched by the Reality? Oxid Med Cell Longev 2016, 7857186. [PubMed: 26881038]

Huebner JL, Seifer DR & Kraus VB. (2007). A longitudinal analysis of serum cytokines in the Hartley guinea pig model of osteoarthritis. Osteoarthritis Cartilage 15, 354–356. [PubMed: 17208467]

Hybertson BM, Gao B, Bose S & McCord JM. (2019). Phytochemical Combination PB125 Activates the Nrf2 Pathway and Induces Cellular Protection against Oxidative Injury. Antioxidants (Basel) 8, 119. [PubMed: 31058853]

Hybertson BM, Gao B, Bose SK & McCord JM. (2011). Oxidative stress in health and disease: the therapeutic potential of Nrf2 activation. Mol Aspects Med 32, 234–246. [PubMed: 22020111]

US Bone and Joint Initiative. (2020). The Burden of Musculoskeletal Diseases in the United States (BMUS).

Islam H, Bonafiglia JT, Turnbull PC, Simpson CA, Perry CGR & Gurd BJ. (2020). The impact of acute and chronic exercise on Nrf2 expression in relation to markers of mitochondrial biogenesis in human skeletal muscle. Eur J Appl Physiol 120, 149–160. [PubMed: 31707475]

Jacques M, Kuang J, Bishop DJ, Yan X, Alvarez-Romero J, Munson F, Garnham A, Papadimitriou I, Voisin S & Eynon N. (2020). Mitochondrial respiration variability and simulations in human skeletal muscle: The Gene SMART study. Faseb J 34, 2978–2986. [PubMed: 31919888]

Jimenez PA, Glasson SS, Trubetskoy OV & Haimes HB. (1997). Spontaneous osteoarthritis in Dunkin Hartley guinea pigs: histologic, radiologic, and biochemical changes. Lab Anim Sci 47, 598–601. [PubMed: 9433695]

Karakelides H, Irving BA, Short KR, O'Brien P & Nair KS. (2010). Age, obesity, and sex effects on insulin sensitivity and skeletal muscle mitochondrial function. Diabetes 59, 89–97. [PubMed: 19833885]

Katsanos CS, Kobayashi H, Sheffield-Moore M, Aarsland A & Wolfe RR. (2006). A high proportion of leucine is required for optimal stimulation of the rate of muscle protein synthesis by essential amino acids in the elderly. Am J Physiol Endocrinol Metab 291, E381–387. [PubMed: 16507602]

Kaushik S & Cuervo AM. (2015). Proteostasis and aging. Nat Med 21, 1406–1415. [PubMed: 26646497]

Kemmler W, Teschler M, Goisser S, Bebenek M, von Stengel S, Bollheimer LC, Sieber CC & Freiberger E. (2015). Prevalence of sarcopenia in Germany and the corresponding effect of osteoarthritis in females 70 years and older living in the community: results of the FORMoSA study. Clin Interv Aging 10, 1565–1573. [PubMed: 26491272]

Kent-Braun JA & Ng AV. (2000). Skeletal muscle oxidative capacity in young and older women and men. J Appl Physiol (1985) 89, 1072–1078. [PubMed: 10956353]

Kitaoka Y, Tamura Y, Takahashi K, Takeda K, Takemasa T & Hatta H. (2019). Effects of Nrf2 deficiency on mitochondrial oxidative stress in aged skeletal muscle. Physiol Rep 7, e13998. [PubMed: 30756520]

Kobayashi EH, Suzuki T, Funayama R, Nagashima T, Hayashi M, Sekine H, Tanaka N, Moriguchi T, Motohashi H, Nakayama K & Yamamoto M. (2016). Nrf2 suppresses macrophage inflammatory response by blocking proinflammatory cytokine transcription. Nat Commun 7, 11624. [PubMed: 27211851]

Konopka AR, Asante A, Lanza IR, Robinson MM, Johnson ML, Dalla Man C, Cobelli C, Amols MH, Irving BA & Nair KS. (2015). Defects in mitochondrial efficiency and H2O2 emissions in obese women are restored to a lean phenotype with aerobic exercise training. Diabetes 64, 2104–2115. [PubMed: 25605809]

Konopka AR, Laurin JL, Musci RV, Wolff CA, Reid JJ, Biela LM, Zhang Q, Peelor FF 3rd, Melby CL, Hamilton KL & Miller BF. (2017). Influence of Nrf2 activators on subcellular skeletal muscle protein and DNA synthesis rates after 6 weeks of milk protein feeding in older adults. Geroscience 39, 175–186. [PubMed: 28283797]

Kovac S, Angelova PR, Holmstrom KM, Zhang Y, Dinkova-Kostova AT & Abramov AY. (2015). Nrf2 regulates ROS production by mitochondria and NADPH oxidase. Biochim Biophys Acta 1850, 794–801. [PubMed: 25484314]

Krul M, van der Wouden JC, Schellevis FG, van Suijlekom-Smit LW & Koes BW. (2009). Musculoskeletal problems in overweight and obese children. Ann Fam Med 7, 352–356. [PubMed: 19597173]

Kruse SE, Karunadharma PP, Basisty N, Johnson R, Beyer RP, MacCoss MJ, Rabinovitch PS & Marcinek DJ. (2016). Age modifies respiratory complex I and protein homeostasis in a muscle type-specific manner. Aging Cell 15, 89–99. [PubMed: 26498839]

Kubo E, Chhunchha B, Singh P, Sasaki H & Singh DP. (2017). Sulforaphane reactivates cellular antioxidant defense by inducing Nrf2/ARE/Prdx6 activity during aging and oxidative stress. Sci Rep 7, 14130. [PubMed: 29074861]

Kumaran S, Panneerselvam KS, Shila S, Sivarajan K & Panneerselvam C. (2005). Age-associated deficit of mitochondrial oxidative phosphorylation in skeletal muscle: role of carnitine and lipoic acid. Mol Cell Biochem 280, 83–89. [PubMed: 16311908]

Lee SY, Ro HJ, Chung SG, Kang SH, Seo KM & Kim DK. (2016). Low Skeletal Muscle Mass in the Lower Limbs Is Independently Associated to Knee Osteoarthritis. PLoS One 11, e0166385. [PubMed: 27832208]

Loeser RF. (2010). Age-related changes in the musculoskeletal system and the development of osteoarthritis. Clin Geriatr Med 26, 371–386. [PubMed: 20699160]

McCord JM, Hybertson BM, Cota-Gomez A & Gao B. (2021). Nrf2 Activator PB125(R) as a Carnosic Acid-Based Therapeutic Agent against Respiratory Viral Diseases, including COVID-19. Free Radic Biol Med.

McElroy GS, Reczek CR, Reyfman PA, Mithal DS, Horbinski CM & Chandel NS. (2020). NAD+ Regeneration Rescues Lifespan, but Not Ataxia, in a Mouse Model of Brain Mitochondrial Complex I Dysfunction. Cell Metab 32, 301–308.e306. [PubMed: 32574562]

Merder-Coskun D, Uzuner A, Kenis-Coskun O, Celenlioglu AE, Akman M & Karadag-Saygi E. (2017). Relationship between obesity and musculoskeletal system findings among children and adolescents. Turk J Phys Med Rehabil 63, 207–214. [PubMed: 31453456]

Merry TL & Ristow M. (2016). Nuclear factor erythroid-derived 2-like 2 (NFE2L2, Nrf2) mediates exercise-induced mitochondrial biogenesis and the anti-oxidant response in mice. J Physiol 594, 5195–5207. [PubMed: 27094017]

Miller BF, Baehr LM, Musci RV, Reid JJ, Peelor FF 3rd, Hamilton KL & Bodine SC. (2019). Muscle-specific changes in protein synthesis with aging and reloading after disuse atrophy. J Cachexia Sarcopenia Muscle 10, 1195–1209. [PubMed: 31313502]

Miller BF, Drake JC, Naylor B, Price JC & Hamilton KL. (2014). The measurement of protein synthesis for assessing proteostasis in studies of slowed aging. Ageing Res Rev 18, 106–111. [PubMed: 25283966]

Miller BF, Reid JJ, Price JC, Lin H-JL, Atherton PJ & Smith K. (2020). Cores of Reproducibility in Physiology: The Use of Deuterated Water for the Measurement of Protein Synthesis. J Appl Physiol.

Miller BF, Robinson MM, Bruss MD, Hellerstein M & Hamilton KL. (2012). A comprehensive assessment of mitochondrial protein synthesis and cellular proliferation with age and caloric restriction. Aging Cell 11, 150–161. [PubMed: 22081942]

Miller BF, Robinson MM, Reuland DJ, Drake JC, Peelor FF 3rd, Bruss MD, Hellerstein MK & Hamilton KL. (2013). Calorie restriction does not increase short-term or long-term protein synthesis. J Gerontol A Biol Sci Med Sci 68, 530–538. [PubMed: 23105041]

Miller BF, Wolff CA, Peelor FF 3rd, Shipman PD & Hamilton KL. (2015). Modeling the contribution of individual proteins to mixed skeletal muscle protein synthetic rates over increasing periods of label incorporation. J Appl Physiol (1985) 118, 655–661. [PubMed: 25593288]

Minton DM, Elliehausen CJ, Javors MA, Santangello KS & Konopka AR. (2021). Rapamycin induced hypergllycemia is associated with exacerbated age-related osteoarthritis. bioRxiv.

Miotto PM, McGlory C, Holloway TM, Phillips SM & Holloway GP. (2018). Sex differences in mitochondrial respiratory function in human skeletal muscle. Am J Physiol Regul Integr Comp Physiol 314, R909–R915. [PubMed: 29513564]

Musci RV, Hamilton KL & Linden MA. (2019). Exercise-Induced Mitohormesis for the Maintenance of Skeletal Muscle and Healthspan Extension. Sports (Basel) 7, 170 118. [PubMed: 31336753]

Musci RV, Hamilton KL & Miller BF. (2018). Targeting mitochondrial function and proteostasis to mitigate dynapenia. Eur J Appl Physiol 118, 1–9. [PubMed: 28986697]

Musci RV, Walsh MA, Konopka AR, Wolff CA, Peelor FF 3rd, Reiser RF 2nd, Santangelo KS & Hamilton KL. (2020). The Dunkin Hartley Guinea Pig Is a Model of Primary Osteoarthritis That Also Exhibits Early Onset Myofiber Remodeling That Resembles Human Musculoskeletal Aging. Front Physiol 11, 571372. [PubMed: 33192568]

Muthusamy VR, Kannan S, Sadhaasivam K, Gounder SS, Davidson CJ, Boeheme C, Hoidal JR, Wang L & Rajasekaran NS. (2012). Acute exercise stress activates Nrf2/ARE signaling and promotes antioxidant mechanisms in the myocardium. Free Radic Biol Med 52, 366–376. [PubMed: 22051043]

Newman LE & Shadel GS. (2018). Pink1/Parkin link inflammation, mitochondrial stress, and neurodegeneration. J Cell Biol 217, 3327–3329. [PubMed: 30154188]

Noack J, Brambilla Pisoni G & Molinari M. (2014). Proteostasis: bad news and good news from the endoplasmic reticulum. Swiss Med Wkly 144, w14001. [PubMed: 25144910]

Noehren B, Kosmac K, Walton RG, Murach KA, Lyles MF, Loeser RF, Peterson CA & Messier SP. (2018). Alterations in quadriceps muscle cellular and molecular properties in adults with moderate knee osteoarthritis. Osteoarthritis Cartilage 26, 1359–1368. [PubMed: 29800621]

Ogawa Y, Kaneko Y, Sato T, Shimizu S, Kanetaka H & Hanyu H. (2018). Sarcopenia and Muscle Functions at Various Stages of Alzheimer Disease. Front Neurol 9, 710. [PubMed: 30210435]

Ostrom EL & Traustadottir T. (2020). Aerobic exercise training partially reverses the impairment of Nrf2 activation in older humans. Free Radic Biol Med 160, 418–432. [PubMed: 32866619]

Pesta D & Gnaiger E. (2011). High-Resolution Respirometry: OXPHOS Protocols for Human Cells and Permeabilized Fibers from Small Biopsies of Human Muscle. Methods Mol Biology Clifton N J 810, 25–58.

Piantadosi CA, Carraway MS, Babiker A & Suliman HB. (2008). Heme oxygenase-1 regulates cardiac mitochondrial biogenesis via Nrf2-mediated transcriptional control of nuclear respiratory factor-1. Circ Res 103, 1232–1240. [PubMed: 18845810]

Quesenberry KF, Orcutt CJ, Mans C & Carpenter JW. (2021). Ferrets, Rabbits, and Rodents Clinical Medicine and Surgery.

Radakovich LB, Marolf AJ, Culver LA & Santangelo KS. (2019). Calorie restriction with regular chow, but not a high-fat diet, delays onset of spontaneous osteoarthritis in the Hartley guinea pig model. Arthritis Res Ther 21, 145. [PubMed: 31196172]

Ranstam J & Cook JA. (2017). Kaplan-Meier curve. Br J Surg 104, 442. [PubMed: 28199017]

Relaix F, Bencze M, Borok MJ, Der Vartanian A, Gattazzo F, Mademtzoglou D, Perez-Diaz S, Prola A, Reyes-Fernandez PC, Rotini A & Taglietti t. (2021). Perspectives on skeletal muscle stem cells. Nat Commun 12, 692. [PubMed: 33514709]

Reuland DJ, Khademi S, Castle CJ, Irwin DC, McCord JM, Miller BF & Hamilton KL. (2013). Upregulation of phase II enzymes through phytochemical activation of Nrf2 protects cardiomyocytes against oxidant stress. Free Radic Biol Med 56, 102–111. [PubMed: 23201694]

Rieu I, Magne H, Savary-Auzeloux I, Averous J, Bos C, Peyron MA, Combaret L & Dardevet D. (2009). Reduction of low grade inflammation restores blunting of postprandial muscle anabolism and limits sarcopenia in old rats. J Physiol 587, 5483–5492. [PubMed: 19752122]

Rivas DA, McDonald DJ, Rice NP, Haran PH, Dolnikowski GG & Fielding RA. (2016). Diminished anabolic signaling response to insulin induced by intramuscular lipid accumulation is associated with inflammation in aging but not obesity. American journal of physiology Regulatory, integrative and comparative physiology 310, R561 569. [PubMed: 26764052]

Robinson MM, Sather BK, Burney ER, Ehrlicher SE, Stierwalt HD, Franco MC & Newsom SA. (2019). Robust intrinsic differences in mitochondrial respiration and H 2 O 2 emission between L6 and C2C12 cells. Am J Physiol-cell Ph 317, C339–C347.

Robinson MM, Turner SM, Hellerstein MK, Hamilton KL & Miller BF. (2011). Long-term synthesis rates of skeletal muscle DNA and protein are higher during aerobic training in older humans than in sedentary young subjects but are not altered by protein supplementation. Faseb J 25, 3240–3249. [PubMed: 21613572]

Rolfe DF & Brown GC. (1997). Cellular energy utilization and molecular origin of standard metabolic rate in mammals. Physiol Rev 77, 731–758. [PubMed: 9234964]

Roux CH, Guillemin F, Boini S, Longuetaud F, Arnault N, Hercberg S & Briancon S. (2005). Impact of musculoskeletal disorders on quality of life: an inception cohort study. Ann Rheum Dis 64, 606–611. [PubMed: 15576417]

Ryu D, Mouchiroud L, Andreux PA, Katsyuba E, Moullan N, Nicolet-Dit-Felix AA, Williams EG, Jha P, Lo Sasso G, Huzard D, Aebischer P, Sandi C, Rinsch C & Auwerx J. (2016). Urolithin A induces mitophagy and prolongs lifespan in C. elegans and increases muscle function in rodents. Nat Med 22, 879–888. [PubMed: 27400265]

Safdar A, deBeer J & Tarnopolsky MA. (2010). Dysfunctional Nrf2-Keap1 redox signaling in skeletal muscle of the sedentary old. Free Radic Biol Med 49, 1487–1493. [PubMed: 20708680]

Salvestrini V, Sell C & Lorenzini A. (2019). Obesity May Accelerate the Aging Process. Front Endocrinol (Lausanne) 10, 266. [PubMed: 31130916]

Santangelo KS, Kaeding AC, Baker SA & Bertone AL. (2014). Quantitative Gait Analysis Detects Significant Differences in Movement between Osteoarthritic and Nonosteoarthritic Guinea Pig

Strains before and after Treatment with Flunixin Meglumine. Arthritis 2014, 503519 503518. [PubMed: 24963402]

Santangelo KS, Pieczarka EM, Nuovo GJ, Weisbrode SE & Bertone AL. (2011). Temporal expression and tissue distribution of interleukin-1beta in two strains of guinea pigs with varying propensity for spontaneous knee osteoarthritis. Osteoarthritis Cartilage 19, 439–448. [PubMed: 21251992]

Santra M, Dill KA & de Graff AMR. (2019). Proteostasis collapse is a driver of cell aging and death. Proc Natl Acad Sci U S A 116, 22173–22178. [PubMed: 31619571]

Shafiee G, Keshtkar A, Soltani A, Ahadi Z, Larijani B & Heshmat R. (2017). Prevalence of sarcopenia in the world: a systematic review and meta- analysis of general population studies. J Diabetes Metab Disord 16, 21. [PubMed: 28523252]

Short KR, Bigelow ML, Kahl J, Singh R, Coenen-Schimke J, Raghavakaimal S & Nair KS. (2005). Decline in skeletal muscle mitochondrial function with aging in humans. Proc Natl Acad Sci U S A 102, 5618–5623. [PubMed: 15800038]

Sieljacks P, Wang J, Groennebaek T, Rindom E, Jakobsgaard JE, Herskind J, Gravholt A, Moller AB, Musci RV, de Paoli FV, Hamilton KL, Miller BF & Vissing K. (2019). Six Weeks of Low-Load Blood Flow Restricted and High-Load Resistance Exercise Training Produce Similar Increases in Cumulative Myofibrillar Protein Synthesis and Ribosomal Biogenesis in Healthy Males. Front Physiol 10, 649. [PubMed: 31191347]

Smiles WJ, Churchward-Venne TA, van Loon LJC, Hawley JA & Camera DM. (2019). A single bout of strenuous exercise overcomes lipid-induced anabolic resistance to protein ingestion in overweight, middle-aged men. Faseb J 33, 7009–7017. [PubMed: 30840513]

Sorrentino V, Romani M, Mouchiroud L, Beck JS, Zhang H, D'Amico D, Moullan N, Potenza F, Schmid AW, Rietsch S, Counts SE & Auwerx J. (2017). Enhancing mitochondrial proteostasis reduces amyloid-beta proteotoxicity. Nature 552, 187–193. [PubMed: 29211722]

Stolle S, Ciapaite J, Reijne AC, Talarovicova A, Wolters JC, Aguirre-Gamboa R, van der Vlies P, de Lange K, Neerincx PB, van der Vries G, Deelen P, Swertz MA, Li Y, Bischoff R, Permentier HP, Horvatovitch PL, Groen AK, van Dijk G, Reijngoud DJ & Bakker BM. (2018). Running-wheel activity delays mitochondrial respiratory flux decline in aging mouse muscle via a post-transcriptional mechanism. Aging Cell 17, e12700 12711. [PubMed: 29120091]

Strong R, Miller RA, Antebi A, Astle CM, Bogue M, Denzel MS, Fernandez E, Flurkey K, Hamilton KL, Lamming DW, Javors MA, de Magalhaes JP, Martinez PA, McCord JM, Miller BF, Muller M, Nelson JF, Ndukum J, Rainger GE, Richardson A, Sabatini DM, Salmon AB, Simpkins JW, Steegenga WT, Nadon NL & Harrison DE. (2016). Longer lifespan in male mice treated with a weakly estrogenic agonist, an antioxidant, an alpha-glucosidase inhibitor or a Nrf2-inducer. Aging Cell 15, 872–884. [PubMed: 27312235]

Sullivan GM & Feinn R. (2012). Using Effect Size-or Why the P Value Is Not Enough. J Grad Med Educ 4, 279–282. [PubMed: 23997866]

Szczepanowska K & Trifunovic A. (2021). Tune instead of destroy: How proteolysis keeps OXPHOS in shape. Bba-Bioenergetics 1862, 148365. [PubMed: 33417924]

Tonge DP, Bardsley RG, Parr T, Maciewicz RA & Jones SW. (2013). Evidence of changes to skeletal muscle contractile properties during the initiation of disease in the ageing guinea pig model of osteoarthritis. Longev Heal 2, 15.

Trappe TA, White F, Lambert CP, Cesar D, Hellerstein M & Evans WJ. (2002). Effect of ibuprofen and acetaminophen on postexercise muscle protein synthesis. Am J Physiol Endocrinol Metab 282, E551–556. [PubMed: 11832356]

Vaananen HK. (1993). Mechanism of bone turnover. Ann Med 25, 353–359. [PubMed: 8217101]

Volpi E, Sheffield-Moore M, Rasmussen BB & Wolfe RR. (2001). Basal muscle amino acid kinetics and protein synthesis in healthy young and older men. JAMA 286, 1206–1212. [PubMed: 11559266]

Wahl D, Moreno JA, Santangello KS, Zhang Q, Afzali MF, Walsh MA, Musci RV, Cavalier AN, Hamilton KL & LaRocca TJ. (2022). Non-Transgenic Guinea Pig Strains Exhibit Hallmarks of Human Brain Aging and Alzheimer's Disease. Journal of Gerontology: Biological Sciences.

Walston J, Hadley EC, Ferrucci L, Guralnik JM, Newman AB, Studenski SA, Ershler WB, Harris T & Fried LP. (2006). Research agenda for frailty in older adults: toward a better understanding

of physiology and etiology: summary from the American Geriatrics Society/National Institute on Aging Research Conference on Frailty in Older Adults. J Am Geriatr Soc 54, 991–1001. [PubMed: 16776798]

Wang C, Chan JS, Ren L & Yan JH. (2016). Obesity Reduces Cognitive and Motor Functions across the Lifespan. Neural Plast 2016, 2473081. [PubMed: 26881095]

Waterlow JC. (1984). Protein turnover with special reference to man. Q J Exp Physiol 69, 409–438. [PubMed: 6382379]

Watson PJ, Hall LD, Malcolm A & Tyler JA. (1996). Degenerative joint disease in the guinea pig. Use of magnetic resonance imaging to monitor progression of bone pathology. Arthritis Rheum 39, 1327–1337. [PubMed: 8702441]

Wilkes EA, Selby AL, Atherton PJ, Patel R, Rankin D, Smith K & Rennie MJ. (2009). Blunting of insulin inhibition of proteolysis in legs of older subjects may contribute to age-related sarcopenia. Am J Clin Nutr 90, 1343–1350. [PubMed: 19740975]

Williams GR, Deal AM, Muss HB, Weinberg MS, Sanoff HK, Guerard EJ, Nyrop KA, Pergolotti M & Shachar SS. (2018). Frailty and skeletal muscle in older adults with cancer. J Geriatr Oncol 9, 68–73. [PubMed: 28844849]

Wolff CA, Lawrence MM, Porter H, Zhang Q, Reid JJ, Laurin JL, Musci RV, Linden MA, Peelor FF 3rd, Wren JD, Creery JS, Cutler KJ, Carson RH, Price JC, Hamilton KL & Miller BF. (2021). Sex differences in changes of protein synthesis with rapamycin treatment are minimized when metformin is added to rapamycin. Geroscience 43, 809–828. [PubMed: 32761290]

Wolff CA, Reid JJ, Musci RV, Linden MA, Konopka AR, Peelor FF, Miller BF & Hamilton KL. (2019). Differential Effects of Rapamycin and Metformin in Combination with Rapamycin on Mechanisms of Proteostasis in Cultured Skeletal Myotubes. Journals Gerontology Ser 128, 412.

Yoshimura Y, Wakabayashi H, Yamada M, Kim H, Harada A & Arai H. (2017). Interventions for Treating Sarcopenia: A Systematic Review and Meta-Analysis of Randomized Controlled Studies. J Am Med Dir Assoc 18, 553 e551–553 e516.

Yu C & Xiao JH. (2021). The Keap1-Nrf2 System: A Mediator between Oxidative Stress and Aging. Oxid Med Cell Longev 2021, 6635460. [PubMed: 34012501]

Zampieri S, Pietrangelo L, Loefler S, Fruhmann H, Vogelauer M, Burggraf S, Pond A, Grim-Stieger M, Cvecka J, Sedliak M, Tirpakova V, Mayr W, Sarabon N, Rossini K, Barberi L, De Rossi M, Romanello V, Boncompagni S, Musaro A, Sandri M, Protasi F, Carraro U & Kern H. (2015). Lifelong physical exercise delays age-associated skeletal muscle decline. J Gerontol A Biol Sci Med Sci 70, 163–173. [PubMed: 24550352]

Zangarelli A, Chanseaume E, Morio B, Brugere C, Mosoni L, Rousset P, Giraudet C, Patrac V, Gachon P, Boirie Y & Walrand S. (2006). Synergistic effects of caloric restriction with maintained protein intake on skeletal muscle performance in 21-month-old rats: a mitochondria-mediated pathway. Faseb J 20, 2439–2450. [PubMed: 17142793]

Key Points Summary

- Aside from exercise, there are no effective interventions for musculoskeletal decline, which begins in the fifth decade of life and contributes to disability and cardiometabolic diseases.
- Targeting both mitochondrial dysfunction and impaired protein homeostasis (proteostasis), which contribute to the age and disease process, may mitigate the progressive decline in overall musculoskeletal function (e.g. gait, strength).
- A potential intervention to target disease drivers is to stimulate Nrf2 activation, which leads to the transcription of genes responsible for redox homeostasis, proteome maintenance, and mitochondrial energetics.
- Here, we tested a purported phytochemical Nrf2 activator, PB125, to improve mitochondrial function and proteostasis in male and female Hartley guinea pigs, which are a model for musculoskeletal aging.
- PB125 improved mitochondrial respiration and attenuated disease- and age-related declines in skeletal muscle protein synthesis, a component of proteostasis, in both male and female Hartley guinea pigs.

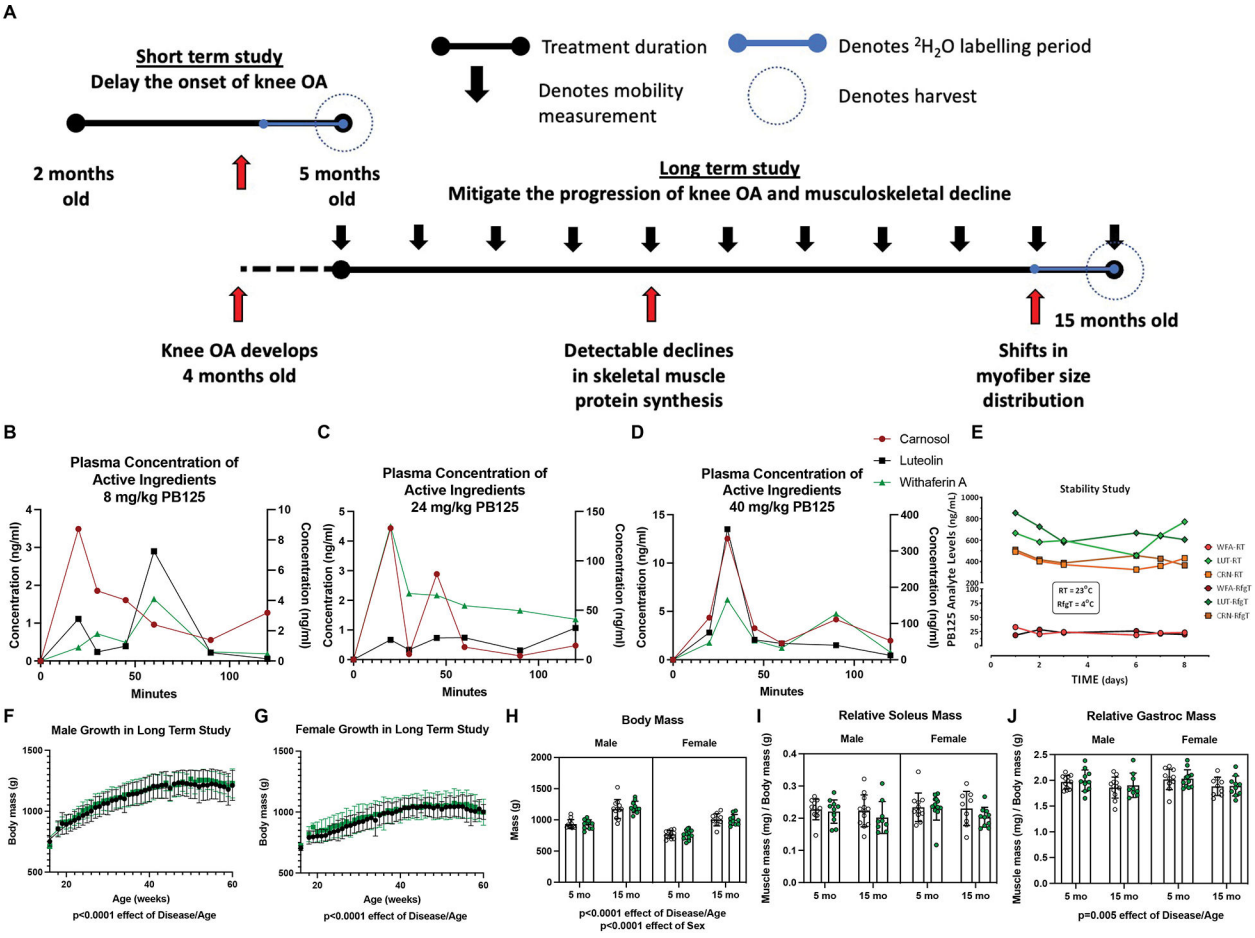

Figure 1.

Study Design, PB125 plasma concentration, and anthropometric data. There were two cohorts of guinea pigs in this study **(A)**. The first cohort was treated with PB125 or vehicle control from 2 mo to 5 mo, an age range during which knee OA begins developing. The second cohort was treated from 5 mo to 15 mo of age, an age range after the onset of knee OA and during which detectable declines in musculoskeletal quality arise. In the final 30 days of each study, a bolus I.P. injection of ^2H_2O was administered and ^2H_2O was mixed in drinking for measurement of protein synthesis. A portion of the soleus was harvested for mitochondrial respirometry assessments. Another portion of the soleus as well as a portion of the gastrocnemius was harvested for isotopic measurements. Comparisons between 5 mo and 15 mo guinea pigs were made between the cohorts at the day of harvest. Longitudinal weight and mobility data were acquired from the second cohort. The plasma concentrations of luteolin, carnosol, and withaferin A after dosing guinea pigs with 8 **(B)**, 24 **(C)**, or 40 **(D)** mg/kg of PB125 from 0 to 120 min. The plasma concentrations of luteolin and withaferin A are on the primary Y-axis and carnosol is on the secondary Y-axis. The stability of the phytochemical components suspended in OraSweet vehicle at room temperature and in 4°C **(E)**. Growth charts for male **(F)** and female **(G)** guinea pigs (n=28 for each sex). There was a significant effect of Disease/Age ($p<0.0001$) and Sex ($p<0.0001$) on guinea pig body mass (n=88) **(H)**. There was no effect of Disease/Age in relative soleus mass (mg of muscle/g

of body mass) (n=86) **(I);** however, there was a significant (p=0.005) negative effect of Disease/Age on the gastrocnemius (n=86) **(J)**

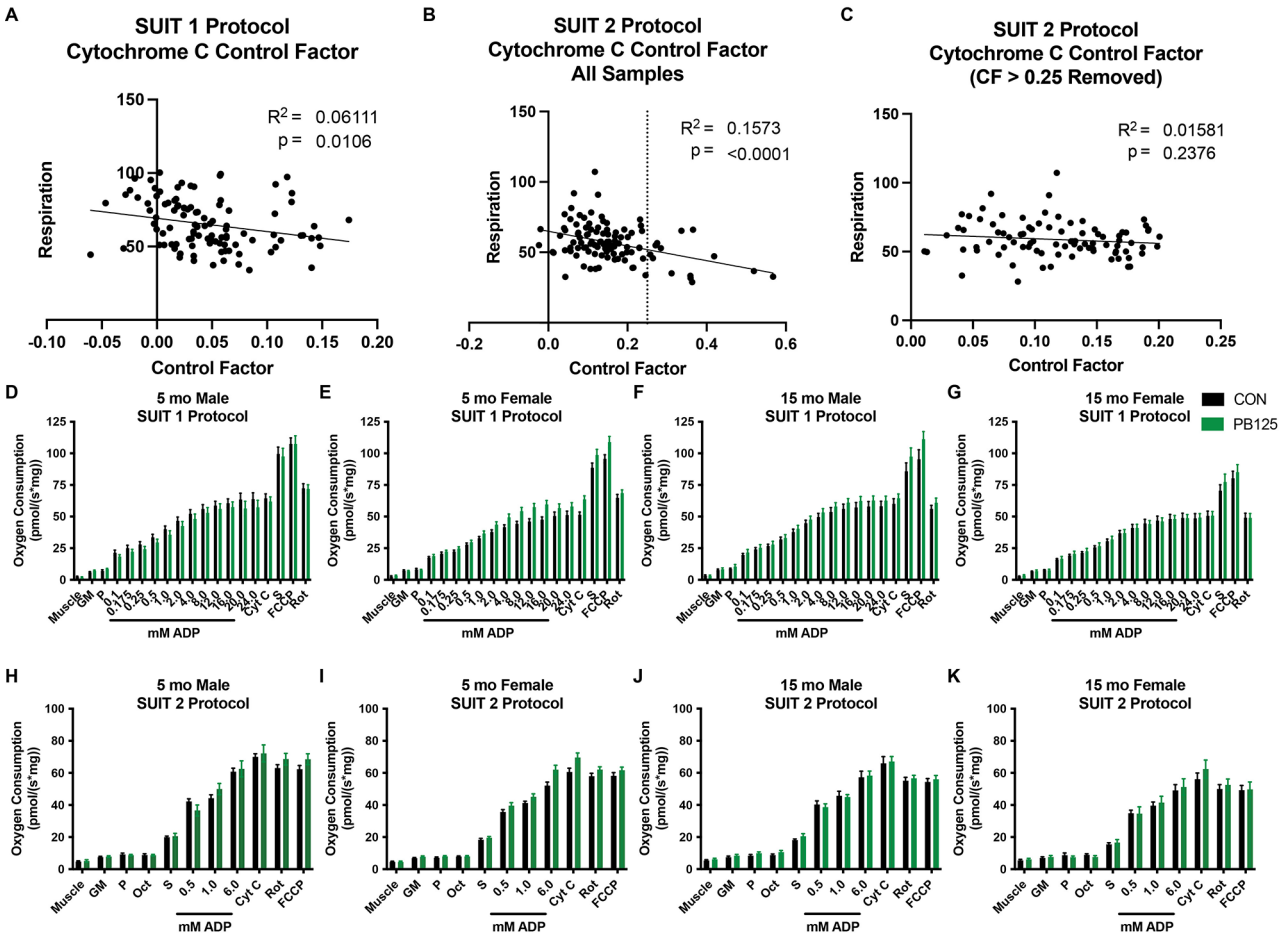

Figure 2.

Cytochrome C Control Factor Scatterplots and SUIT Protocol overviews. Scatterplots and regression line relating Cytochrome C Control Factor to coupled respiration in Suit 1 (n=107) **(A)** and Suit 2 before (n=107) **(B)** and after (n=94) **(C)** a limit of 0.25 (dotted line drawn on **B**) was implemented to establish O2K trials to exclude due to over permeabilization. Graphs summarizing the age/sex/treatment groups of the SUIT 1 protocol (**D – G)** and SUIT 2 protocol (**H – K)**. Statistics were not conducted on the data grouped in this manner.

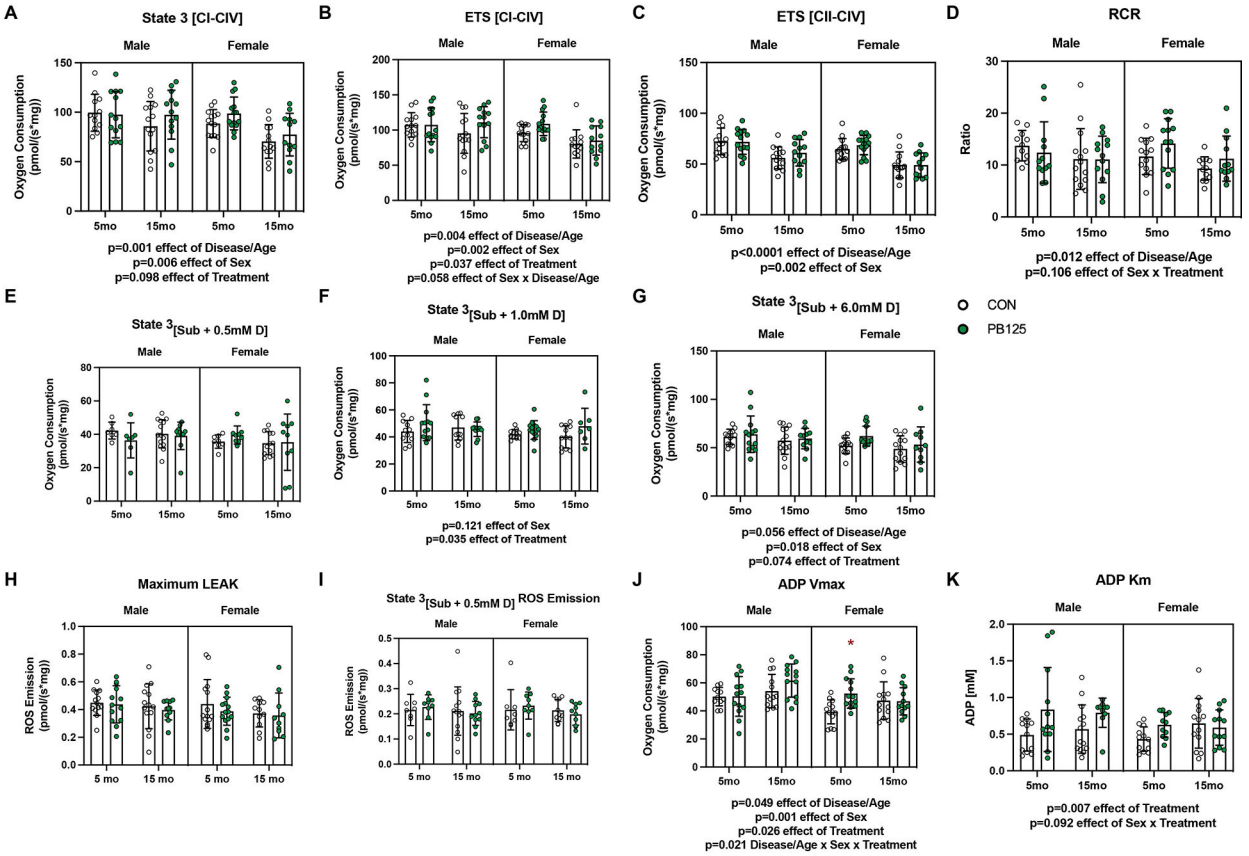

Figure 3.

Disease/Age-, Sex-, and Treatment-related differences in mitochondrial respiration from SUIT 1 & 2 protocols. There was a significant negative effect of Disease/Age on State $3_{[CI-CIV]}$ respiration (Cohen's d=0.731, p=0.001). Female guinea pigs had lower levels of respiration compared to males (Cohen's d=0.653, p=0.006). Treatment did not significantly increase respiration (Cohen's d=0.357, p=0.098) (n=105) **(A)**. Electron transport system capacity ($ETS_{[CI-CIV]}$) significantly decreased with Disease/Age (Cohen's d=0.680, p=0.004) and was lower in females (Cohen's d=0.735, p=0.002). PB125 treatment increased respiration (Cohen's d=0.438, p=0.037). The interaction effect between Sex and Disease/Age was not significant (p=0.058) (n=107) **(B)**. There was a significant decrease in Complex II – IV uncoupled respiration with age (Cohen's d=1.388, p<0.0001), but there was no effect of Treatment (Cohen's d=0.175, p=0.369). Female guinea pigs had lower respiration compared to male guinea pigs (Cohen's d=0.668, p=0.002 effect of Sex) (n=107) **(C)**. Mitochondrial efficiency (RCR) decreased with Disease/Age (p=0.012) and there was no significant interaction (p=0.106) between Sex and Treatment (n=101) **(D)**. There was no difference in fatty acid supported respiration with 0.5 mM ADP between Sex, Disease/Age, or Treatment groups (n=69) **(E)**. Fatty acid supported respiration with 1.0 mM ADP was higher in PB125 treated guinea pigs (Cohen's d=0.519, p=0.035 effect of Treatment), but the effect of Sex or Disease/Age was not significant (p=0.121, 0.880 respectively) (n=90) **(F)**. At saturating amounts of ADP (6.0 mM), there was no significant effect of Sex on fatty acid supported respiration (Cohen's d=0.413, p=0.070) or PB125 treatment (Cohen's d=0.402,

p=0.077) (n=90) **(G)**. PB125 treatment had no effect on ROS emission during LEAK (i.e. State 2 respiration) (n=86) **(H)** or State 3 respiration in the presence of sub-saturating amounts (0.5 mM) of ADP (n=66) **(I)**. There was a Disease/Age-related increase in ADP Vmax (Cohen's *d*=0.445, p=0.049), though female guinea pigs had a lower Vmax compared males (Cohen's *d*=0.720, p=0.001). PB125 significantly increased ADP Vmax (Cohen's *d*=0.498, p=0.026). Post-hoc analysis revealed PB125 5 mo female had greater ADP Vmax compared to CON 5 mo female guinea pigs (p=0.045) (n=101) **(J)**. There was a significant increase in ADP Km from PB125 treatment (Cohen's *d*=0.669, p=0.007). There was no significant interaction between Sex and Treatment (p=0.092) (n=96) **(K)**.

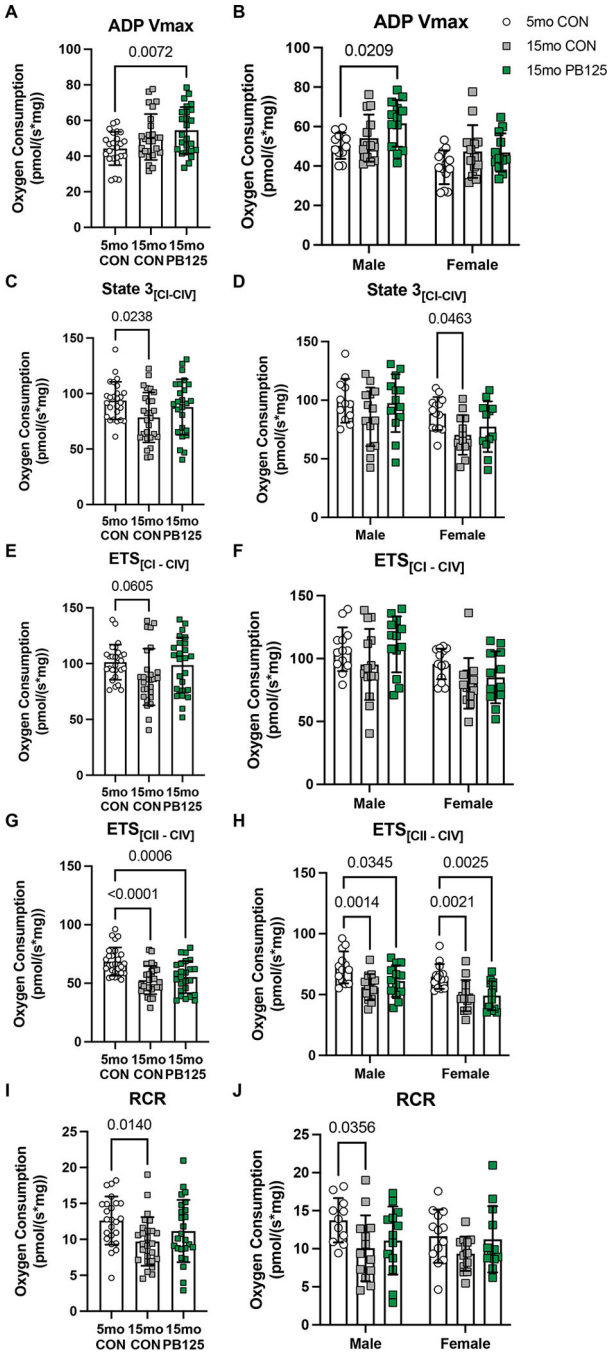

Figure 4.

PB125 attenuates Disease/Age-related declines in mitochondrial respiration. There was no difference in ADP Vmax between 5 mo and 15 mo CON guinea pigs (p=0.109), whereas 15 mo PB125 treated guinea pigs had a higher ADP Vmax than 5 mo CON guinea pigs (Figure 6A; Cohen's *d*=0.869, p=0.007) (n=75) **(A)**. Comparing sex-specific effects, PB125 only had a positive effect in male guinea pigs (p=0.021) (n=75) **(B)**. There was a Disease/Age-related decrease (Cohen's d=0.709, p=0.024) in State $3_{[PGM + S]}$ between CON guinea pigs, though this difference was attenuated in 15 mo PB125 treated guinea pigs (Cohen's

d=0.270, 0.440, compared to 5 mo CON and 15 mo CON) (n=78) **(C)**. The Disease/Age-related decline was only observed in female guinea pigs (p=0.046), and was attenuated by PB125 (p=0.290) (n=78) **(D)**. Uncoupled respiration $ETS_{[CI-CIV]}$ nonsignificantly (Cohen's d=0.600, p=0.061) decreased with Disease/Age, though PB125 attenuated this difference (p=0.875, Cohen's d=0.120, 0.480, compared to 5 mo and 15 mo CON, respectively) (n=79) **(E)**. However, there were no significant differences when sex was considered (n=79) **(F)**. There was a significant decrease (p<0.0001) in $ETS_{[CII-CIV]}$ between 5 mo and 15 mo CON guinea pigs that PB125 did not attenuate (p<0.001) (n=79) **(G)** in either sex (n=79) **(H)**.

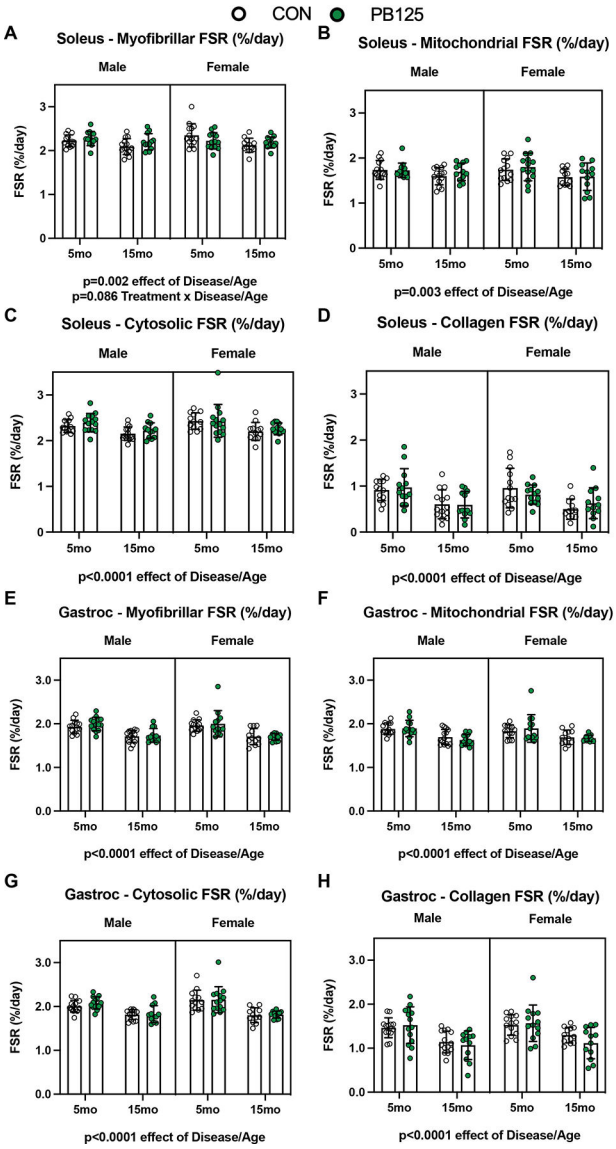

Figure 5.

Fractional synthesis rates (FSR) of both the soleus and gastrocnemius subfractions decreases with Disease/Age. FSR significantly decreased with Disease/Age in all subfractions of the soleus (p=0.002, p=0.003, p<0.0001, p<0.0001 for myofibrillar (n=103) **(A)**, mitochondrial (n=104) **(B)**, cytosolic (n=102) **(C)**, and collagen (n=103) **(D)** subfractions, respectively). 15 mo guinea pigs also had a significant decrease in FSR in every subfraction of gastrocnemius (p<0.0001 for all subfractions) (n=103 for each subfraction except mitochondrial where n=102) **(E – H)**.

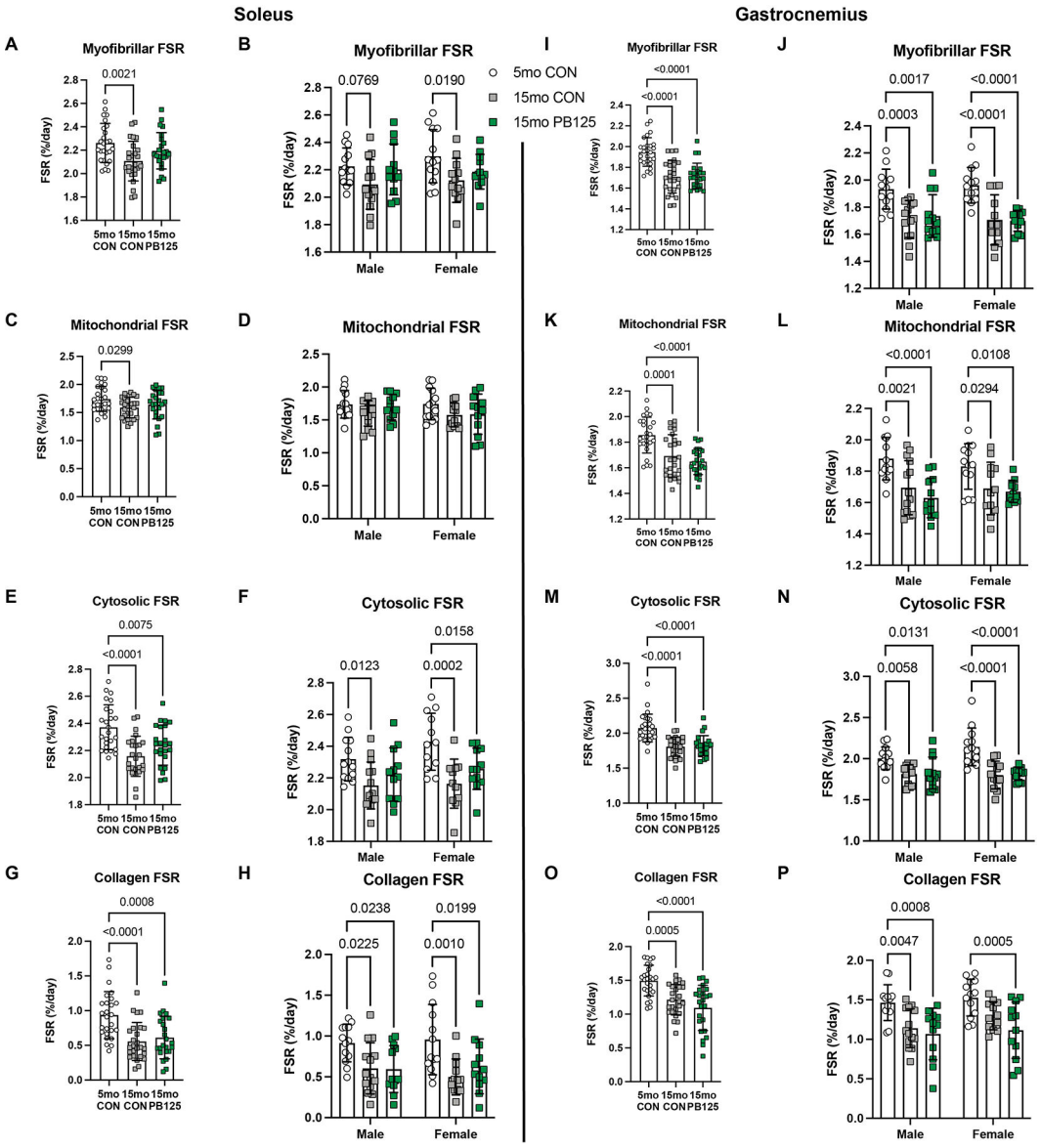

Figure 6.

PB125 treatment attenuates Disease/Age-related declines in FSR in soleus, but not gastrocnemius, subfractions. 15 mo CON guinea pigs had lower FSR in each subfraction of the soleus (p=0.002, p=0.030, p<0.0001, p<0.0001 for the myofibrillar (n=76) **(A)**, mitochondrial (n=76) **(C)**, cytosolic (n=74) **(E)**, and collagen (n=76) **(G)** subfractions, respectively). PB125 attenuated the decline in the myofibrillar **(A)** and mitochondrial **(C)** subfractions, but not in the cytosolic **(E)** or collagen subfractions **(G)**. PB125 attenuated (Cohen's *d*=0.533) the decline in myofibrillar FSR in both males (p=0.920) and females (p=0.166) (n=76) **(B)** and attenuated the decline in cytosolic FSR in males only (p=0.207) (n=74) **(F)**. In the gastrocnemius, 15 mo CON guinea pigs had significantly lower FSR compared to 5 mo CON guinea pigs in each subfraction (p<0.0001 for all subfractions) (n=76, in each subfraction) **(I, K, M, O)**. The FSR of all subfractions of the gastrocnemius in 15 mo PB125 guinea pigs was also significantly lower compared to 5 mo CON guinea

pigs ($p<0.0001$ for all subfractions) (**I, K, M, O)**. This pattern was observed in both male and female guinea pigs (n=76, in each subfraction) **(J, L, N, P)**.

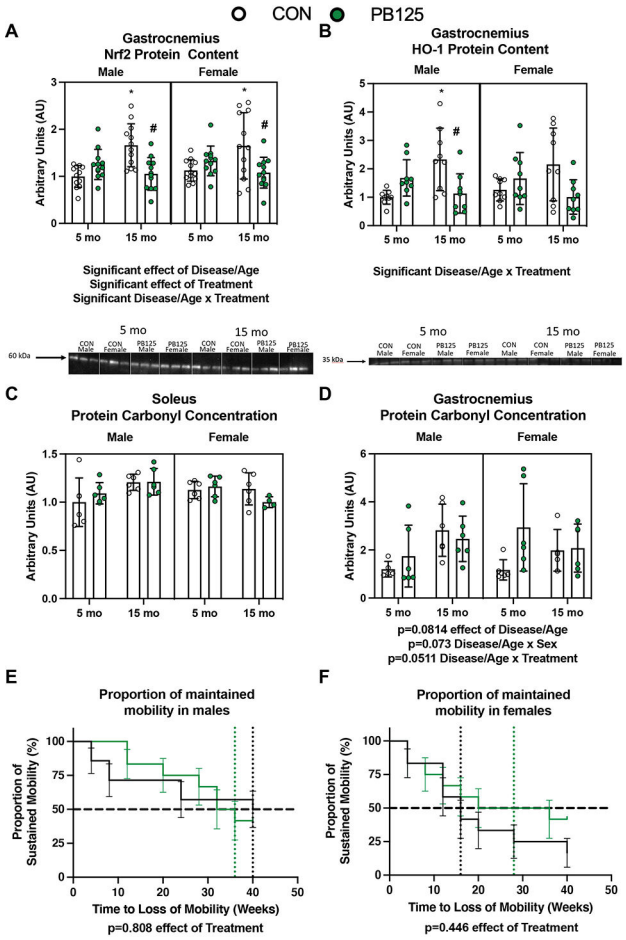

Figure 7.

PB125 influences Nrf2 content but does not significantly change protein carbonylation or mobility. There was no effect of Sex on Nrf2 (n=96) **(A)** or HO-1 (n=72) (**B)** protein content in the gastrocnemius. There was significant effect of Disease/Age and Treatment on Nrf2 protein content Cohen's d=1.462, p=0.025). There was a significant ($p<0.0001$) interaction between Disease/Age and Treatment on both Nrf2 and HO-1 protein content. There was no effect of Disease/Age, Sex, or Treatment on protein carbonyl concentration in the soleus (n=46) **(C)**. There was no (n=46) significant increase (p=0.0814) in protein carbonyl concentration in the gastrocnemius **(D)**. There was a greater proportion of PB125 treated male (n=26) **(E)** and female (n=24) **(F)** guinea pigs that maintained mobility over the course of the study period. However, there was no statistically significant effect of PB125 on the probability of maintaining mobility throughout the course of the study. * denotes significant difference between 5 mo CON; # denotes significant difference between 15 mo CON.

Table 1

Summary of high resolution respirometry experiments using Oroboros Oxygraph-2000. A table highlighting SUIT 1 & 2 protocols used in the study. Further explanations of these respiratory states and measurements can be found in Pesta & Gnaiger, 2011 or at the Oroboros website: www.bioblast.at.

Respiratory State	Substrates	Description
SUIT 1 – A Complex I supported ADP titration evaluating ADP sensitivity as well as maximal respiration, followed with uncoupled respiration.		
State 2 [PGM]	5 mM pyruvate (P), 10 mM glutamate (G), 0.5, mM malate (M)	LEAK respiration in the presence of Complex I substrates. The amount of oxygen consumption as a consequence of protons leaking across the membrane.
State 3 [PGM]	Previous steps + addition of ADP such that [ADP] progressively increased as follows: 0.1 mM, 0.175 mM, 0.25 mM, 1 mM, 2 mM, 4 mM, 8 mM, 12 mM, 20 mM, to 24 mM.	Respiration associated with ATP production. NADH is generated through the oxidation of PGM, donating electrons to Complex I, and creating a proton gradient where ADP is the limiting factor for ATP production. Oxygenconsumption is a consequence of ADP being phosphorylated to ATP. Initial titrations are sub-saturating concentrations of ADP increasing to maximal ADP stimulated respiration.
State 3 [Cyt C]	Previous step + 5 mM Cytochrome C	During permeabilization, the outer membrane of mitochondria can be damaged, resulting in loss of cytochrome C. An increase in oxygen consumption is indicative of cytochrome C release during mechanical or chemical permeabilization.
State 3 [PGM + S]	Previous step + 10 mM succinate (S)	Same as previous step but now both NADH and $FADH_2$ are generated through the oxidation of Complexes I (PGM) and II (S) substrates yielding maximal ADP stimulated respiration.
ETS [CI – CIV]	Previous step + 1.0 mM FCCP	FCCP is a protonophore allowing hydrogen ions through the inner-mitochondrial membrane, uncoupling the proton gradient from ATP production through ATP synthase. This reflects the maximal or reserve capacity of Complexes I – IV, unconstrained from ATP synthase activity.
ETS [CII – CIV]	Previous step + 5 μM rotenone (Rot)	Rotenone is an inhibitor of Complex I. Therefore, uncoupled oxygen consumption is indicative of Complex II – IV capacity.
ROX	2.5 μM Antimycin A (Ama)	Antimycin A inhibits Complex III shutting down the electron transfer pathway. Residual oxygen consumption (ROX) is remaining oxygen consumed from other pathways independent of Complex IV.
SUIT 2 – A protocol measuring coupled and uncoupled respiration as well as ROS emission simultaneously in the presence of fatty acids.		
State 2 [PGM + Oct]	5 mM pyruvate (P), 10 mM glutamate (G), 0.5, mM malate (M), 0.2 mM octanoylcarnitine (Oct)	LEAK respiration in the presence of Complex I and II substrates including both carbohydrates and fatty acids. The amount of oxygen consumption as a consequence of protons leaking across the membrane.
State 2 [PGM + Oct + S]	Previous step + 10 mM succinate (S)	Same as previous step with the addition of the Complex II substrate, succinate (S). This is considered to stimulate maximal LEAK respiration as well as generation of reactive oxygen species (ROS).
State 3 [Sub + 0.5D]	Previous step + 0.5 mM ADP	Respiration associated with ATP production. NADH and $FADH_2$ is generated through the oxidation of PGMS and octanoylcarnitine donating electrons to Complexes I and II, and creating a proton gradient where ADP is the limiting factor for ATP production. The amount of oxygen consumed is from ADP being phosphorylated to ATP with a sub-saturating bolus of ADP.
State 3 [Sub + 1.0D]	Previous step + 0.5 mM ADP	Final concentration of ADP is higher but still sub-saturating stimulated respiration.
State 3 [Sub + 6.0D]	Previous step + 5 mM ADP	Same as previous step, however, the final concentration of ADP (6.0 mM) is a saturating does, maximally stimulating mitochondrial respiration and ATP production.
State 3 [Cyt C]	Previous step + 5 mM Cytochrome C	During permeabilization, the outer membrane of mitochondria can be damaged, resulting in loss of cytochrome C. An increase in oxygen consumption is indicative of cytochrome C release during mechanical or chemical permeabilization. After the addition of cytochrome C, no more assessments of ROS emission were measured.

State 3 [Sub + D − CI]	Previous step + 5 μM rotenone (Rot)	Oxygen consumption reflects stimulated ADP respiration of Complexes II – IV.
ETS [Sub + D − CI]	Previous step + 1.0 mM FCCP	FCCP is a protonophore uncoupling the proton gradient from ATP production through ATP synthase. This is the maximal or reserve capacity of the mitochondria for Complexes II – IV.
Calculated Ratios	**Calculation**	**Description**
Respiratory Control Ratio (RCR)	State 3[PGM] / State 2[PGM]	The ratio of maximally stimulated ATP production to LEAK respiration. Respiratory Control Ratio (RCR) is a metric of mitochondrial coupling efficiency. A higher ratio is indicative of greater mitochondrial efficiency of oxygen consumption coupled to ATP production.
Cytochrome C Control Factor	Suit 1: (State 3 [Cyt C] – State 3 [PGM]) / State 3 [PGM] Suit 2: (State 3 [Cyt C] – State 3 [Sub + 6.0D]) / State 3 [Sub + 6.0D	As a quality control, adding cytochrome C to the SUIT protocol evaluates the extent in which the membrane was damaged and/or over-permeabilized. Refer to Methods: *Mitochondrial Respirometry* and Fig 2A – C for additional information.

Abbreviations: P – pyruvate; G – glutamate; M – malate; S – succinate; Oct – octanoylcarnitine; ADP – adenosine diphosphate; Cyt C – cytochrome C; ATP – adenosine triphosphate; Rot – rotenone; FCCP – Trifluoromethoxy carbonylcyanide phenylhydrazone; Ama – Antimycin A; ETS – electron transport system; Sub – priorly added substrates (i.e. pyruvate, glutamate, malate, octanoylcarnitine, and succinate); CI – Complex I; CII – Complex II; CIII – Complex III; CIV – Complex IV; CV – Complex V or ATP Synthase; ROX – residual oxygen consumption; RCR – respiratory control ratio; NADH – reduced nicotinamide adenine dinucleotide